



Targeting L-Proline Uptake as New Strategy for Anti-chagas Drug Development

Lucía Fargnoli¹, Esteban A. Panozzo-Zénere¹, Lucas Pagura², María Julia Barisón³, Julia A. Cricco², Ariel M. Silber³ and Guillermo R. Labadie^{1,4*}

¹ Facultad de Ciencias Bioquímicas y Farmacéuticas, Instituto de Química de Rosario (IQUIR), Universidad Nacional de Rosario, Rosario, Argentina, ² Instituto de Biología Molecular y Celular de Rosario (IBR), Consejo Nacional de Investigaciones Científicas y Técnicas CONICET–Facultad de Ciencias Bioquímicas y Farmacéuticas, Universidad Nacional de Rosario, Rosario, Argentina, ³ Laboratory of Biochemistry of Tryps-LaBTryps, Departamento de Parasitología, Instituto de Ciências Biomédicas, Universidade de São Paulo, Cidade Universitária, São Paulo, Brazil, ⁴ Departamento de Química Orgánica, Facultad de Ciencias Bioquímicas y Farmacéuticas, Universidad Nacional de Rosario, Rosario, Argentina

OPEN ACCESS

Edited by:

Gildardo Rivera,
National Polytechnic Institute of
Mexico (IPN), Mexico

Reviewed by:

Claudia Masini d'Avila-Levy,
Oswaldo Cruz Foundation
(Fiocruz), Brazil
Juan Diego Maya,
University of Chile, Chile

*Correspondence:

Guillermo R. Labadie
labadie@iquir-conicet.gov.ar

Specialty section:

This article was submitted to
Medicinal and Pharmaceutical
Chemistry,
a section of the journal
Frontiers in Chemistry

Received: 02 April 2020

Accepted: 06 July 2020

Published: 25 August 2020

Citation:

Fargnoli L, Panozzo-Zénere EA,
Pagura L, Barisón MJ, Cricco JA,
Silber AM and Labadie GR (2020)
Targeting L-Proline Uptake as New
Strategy for Anti-chagas Drug
Development. *Front. Chem.* 8:696.
doi: 10.3389/fchem.2020.00696

L-Proline is an important amino acid for the pathogenic protists belonging to *Trypanosoma* and *Leishmania* genera. In *Trypanosoma cruzi*, the etiological agent of Chagas disease, this amino acid is involved in fundamental biological processes such as ATP production, differentiation of the insect and intracellular stages, the host cell infection and the resistance to a variety of stresses. In this study, we explore the L-Proline uptake as a chemotherapeutic target for *T. cruzi*. Novel inhibitors have been proposed containing the amino acid with a linker and a variable region able to block the transporter. A series of sixteen 1,2,3-triazolyl-proline derivatives have been prepared for *in vitro* screening against *T. cruzi* epimastigotes and proline uptake assays. We successfully obtained inhibitors that interfere with the amino acid internalization, which validated our design targeting the metabolite's transport. The presented structures are one of few examples of amino acid transporter inhibitors. The unprecedented application of this strategy on the development of new chemotherapy against Chagas disease, opens a new horizon on antiparasitic drug development against parasitic diseases and other pathologies.

Keywords: Chagas disease, proline uptake, *T. cruzi* epimastigotes, cytotoxicity, target validation

INTRODUCTION

Chagas disease is one of the most neglected infectious disease. It is endemic in the Americas, with 8–10 million people infected and 25 million people at risk (Nunes et al., 2013). The disease is divided in the acute and the chronic phase. The first have a noticeable parasitemia, the absence of humoral response and is largely asymptomatic. The chronic phase has a non-evident parasitemia and a robust IgG response being asymptomatic in 60–70% of the cases (Pérez-Molina and Molina, 2018). The chemotherapy against Chagas disease relies mainly on two drugs introduced more than 40 years ago: Nifurtimox (Nf) and Benznidazole (Bz) (Urbina, 2010). Both drugs are efficient on the acute phase, but in the chronic phase is controversial (Morillo et al., 2015). In addition, severe side effects due to toxicity and the emergence of resistance calls for urgent development of new drugs (Guedes et al., 2011).

Trypanosoma cruzi is a hemoflagellated parasite that causes Chagas disease. This parasite presents a complex life cycle among two kinds of hosts: mammals and reduviid insects,

which transmit the infection. Along its life-cycle at least four stages were clearly identified, epimastigotes (replicative stage) and metacyclic trypomastigotes (infective, non-replicative stage) in the insect and blood stream trypomastigotes and amastigotes (intracellular replicative stage). Also, during its life-cycle the parasite faces different environments and it must adjust its “life-style” including its metabolism to changes in nutrients availability, temperature, together other environmental variables.

Among many other important metabolites, amino acids are particularly relevant for the biology of *T. cruzi*, besides protein synthesis (Marchese et al., 2018), playing fundamental roles in energy management (Pereira et al., 2000) and nitrogen metabolism (Crispim et al., 2018; Girard et al., 2018). When epimastigotes proliferation arrests, there is a metabolic switch from a carbohydrates to an amino acids based metabolism, with a consequent change in the protein expression profile (Barisón et al., 2017; Avila et al., 2018). In fact, it has been demonstrated that amino acids such as proline (Paes et al., 2013), histidine (Barison et al., 2016), and even alanine (Girard et al., 2018), as well as the proline oxidation product P5C (Mantilla et al., 2015), can fuel electrons to the respiratory chain, powering the mitochondrial ATP synthesis (Sylvester and Krassner, 1976; Martins et al., 2009; Paes et al., 2013; Barison et al., 2016). Some neutral amino acids can also function as osmolytes, serving to counteract volume perturbations following a shift in extracellular osmolarity (Rohloff et al., 2003; Silber et al., 2005; Avila et al., 2018).

Particularly, proline is involved in energization of the host-cells invasion by metacyclic trypomastigotes (Martins et al., 2009), as well as growth and differentiation of the insect (Contreras Vt et al., 1988; Tonelli et al., 2004; Silber et al., 2009) and the intracellular stages (Tonelli et al., 2004). Additionally, its accumulation in the parasite cytoplasm provides resistance to oxidative and thermal stress (Tonelli et al., 2004; Magdaleno et al., 2009; Paes et al., 2013; Sayé et al., 2014). The proline availability is mediated by an interplay of the biosynthesis degradation and uptake process (Sylvester and Krassner, 1976; Silber et al., 2002; Magdaleno et al., 2009; Paes et al., 2013; Sayé et al., 2014; Mantilla et al., 2017). In particular, the inhibition of proline uptake by competitive transporter interrupters, diminished the parasites ability to tolerate oxidative imbalance, nutritional stress and to complete the infection cycle (Magdaleno et al., 2009).

Taking the proline uptake as a novel drug target we decided to develop new transporter inhibitors and evaluate their antiproliferative activity against *Trypanosoma cruzi*. These new compounds were initially evaluated on *T. cruzi* epimastigotes, validating their action mechanism by proline transport experiments. A comprehensive analysis of the structure-activity relationship allowed a rational pipeline to design selective metabolite transporter inhibitors.

MATERIALS AND METHODS

Chemistry

General Remarks

Chemical reagents were purchased from commercial suppliers and used without further purification, unless otherwise noted.

Dry, deoxygenated diethyl ether (Et₂O), tetrahydrofuran (THF), and dichloromethane (DCM) were obtained bypassing commercially available pre-dried, oxygen-free solvents through activated alumina columns. DMF was distilled from BaO. Reactions were monitored by thin-layer chromatography (TLC) performed on 0.2 mm Merck silica gel aluminum plates (60F-254) and visualized using ultraviolet light (254 nm) and by potassium permanganate and heat as developing reagents. All reactions were performed under an atmosphere of nitrogen using oven-dried glassware and standard syringe/septa techniques. Column chromatography was performed with silica gel 60 (230–400 mesh). Yields were calculated for material judged homogeneous by thin layer chromatography (TLC) and nuclear magnetic resonance (¹H NMR).

¹H and ¹³C NMR spectra were acquired on a Bruker Avance II 300 MHz (75.13 MHz) using CDCl₃ as solvent. Chemical shifts (δ) were reported in ppm downfield from tetramethylsilane and coupling constants are in hertz (Hz). NMR spectra were obtained at 298 K unless otherwise stated and samples run as a dilute solution of the stated solvent. All NMR spectra were referenced to the residual undeuterated solvent as an internal reference. The following abbreviations were used to explain the multiplicities: s = singlet, d = doublet, t = triplet, q = quartet, m = multiplet, br = broad. Assignment of proton resonances was confirmed by correlated spectroscopy. Electrospray ionization high-resolution mass spectra (ESI-HRMS) were recorded on a Bruker MicroTOF II. IR spectra were obtained using an FT-IR Shimadzu spectrometer and only partial spectral data are listed. Melting points were measured on an Electrothermal 9100 apparatus and are uncorrected.

Experimental Procedures and Spectroscopic Data

Synthesis of N-Propargyl Methyl Prolinate (2)

To a solution of methyl prolinate (200 mg, 1.22 mmol) in 10 mL of Et₂O_(anh), NEt₃ (439 mg, 4.3 mmol) and 80 % propargyl bromide in toluene (263 μL, 2.45 mmol) were added in this order and the reaction mixture was stirred at room temperature for 12 h. The solvent was evaporated, and the crude product was purified by column chromatography in silica gel with increasing ethyl acetate/hexane gradient to yield the expected product as a yellow oil (129 mg, 72 %).

¹H NMR (300 MHz, CDCl₃): δ 3.72 (s, 3H, OCH₃), 3.61–3.55 (m, 2H, C5-H, C2-H), 3.45–3.39 (m, 1H, C6-H), 3.07–3.01 (m, 1H, C6-H), 2.75–2.67 (m, 1H, C5-H), 2.20–2.06 (m, 2H, C7-H and C3-H), 2.08–1.76 (m, 3H, C3-H, C4-H). ¹³C NMR (75 MHz, CDCl₃): δ 173.9 (COO), 78.2 (C), 73.2 (CH), 62.4 (CH), 52.1 (CH₂), 51.9 (OCH₃), 41.1 (CH₂), 29.5 (CH₂), 23.2 (CH₂).

General Procedure for the Cu(I) Mediated 1,3-Dipolar Cycloaddition

N-Propargyl methyl prolinate (1 eq) and the azide (1.1 eq) were suspended in 10 mL/eq of *t*BuOH:H₂O (1:1) and then 1M CuSO₄ solution (0.05 eq) and finally 1M sodium ascorbate solution (0.2 eq) and the mixture stirred overnight at room temperature. Brine was added, and the solution was extracted with dichloromethane. Combined organic extracts

were dried over sodium sulfate and evaporated. Products were purified by column chromatography in silica gel with increasing hexanes/ethyl acetate/methanol gradients.

Methyl ((1-(2-Ethoxy-2-Oxoethyl)-1H-1,2,3-Triazol-4-yl)Methyl)-L-Proline (3a)

Compound **3a** was prepared from 45 mg (0.27 mmol) of N-propargyl methyl proline **1**, following the general procedure for the 1,3-dipolar cycloaddition, affording 66 mg of a yellowish oil in 80 % yield. ^1H NMR (300 MHz, CDCl_3): δ 7.62 (s, 1H, C7-H), 5.09 (d, $J = 2.6$ Hz, 2H, C8-H), 4.20 (q, $J = 7.5$ Hz, 2H, CH_2CH_3), 4.01 (d, $J = 13.8$ Hz, 1H, C6-H), 3.82 (d, $J = 13.8$ Hz, 1H, C6-H), 3.64 (s, 3H, OMe), 3.29 (dd, $J = 8.7, 6.1$ Hz, 1H, C2-H), 3.10–3.04 (m, 1H, C5-H), 2.50 (dt, $J = 8.4$ Hz, $J = 8.2$ Hz, 1H, C5-H), 2.07–1.74 (m, 4H, C3-H and C4-H), 1.23 (t, $J = 7.5$ Hz, 3H, CH_2CH_3). ^{13}C NMR (75 MHz, CDCl_3): δ 174.1 (COO), 166.3 (COO), 144.5 (C6'), 124.4 (C7), 64.4 (C2), 62.4 (CH₂), 53.0 (C5), 52.0 (OCH₃), 50.8 (C8), 48.2 (C6), 29.3 (C3), 23.0 (C4), 14.0 (CH₃). IR (film): ν_{max} 3458, 3439, 2954, 2357, 1732, 1643, 1444, 1217, 1051, 1024, 875, 798, 756 cm^{-1} . ESI-HRMS m/z [M+K]⁺ calcd for $\text{C}_{13}\text{H}_{20}\text{KN}_4\text{O}_4$ 335.1116, found 335.1113.

Methyl ((1-(5-Ethoxy-5-Oxopentyl)-1H-1,2,3-Triazol-4-yl)Methyl)-L-Proline (3b)

Compound **3b** was prepared from 45 mg (0.27 mmol) of N-propargyl methyl proline **1**, following the general procedure for the 1,3-dipolar cycloaddition, affording 63 mg of a yellowish oil in 69 % yield. ^1H NMR (300 MHz, CDCl_3): δ 7.50 (s, 1H, C7-H), 4.38 (d, $J = 2.6$ Hz, 2H, C8-H), 4.09 (q, $J = 7.5$ Hz, 2H, CH_2CH_3), 3.97 (d, $J = 13.8$ Hz, 1H, C6-H), 3.79 (d, $J = 13.8$ Hz, 1H, C6-H), 3.65 (3H, OMe), 3.28 (dd, $J = 8.7, 6.1$ Hz, 1H, C2-H), 3.12–3.07 (m, 1H, C5-H), 2.53–2.45 (m, 1H, C5-H), 2.32–2.08 (m, 6H, CH₂), 1.91–1.76 (m, 4H, C3-H and C4-H), 1.20 (t, $J = 7.5$ Hz, 3H, CH_2CH_3). ^{13}C NMR (75 MHz, CDCl_3): δ 174.4 (C=O), 172.3 (COO), 144.5 (C6'), 122.8 (C7), 64.6 (C2), 60.6 (CH₂CH₃), 53.3 (C5), 51.8 (OCH₃), 49.1 (C8), 48.5 (C6), 30.6 (CH₂), 29.6 (CH₂), 29.3 (C3), 25.4 (C4), 23.0 (CH₂), 14.1 (CH₂CH₃). IR (film): ν_{max} 3437, 3138, 2954, 2358, 1730, 1633, 1444, 1377, 1348, 1274, 1199, 1047, 1028, 854, 802 cm^{-1} . ESI-HRMS m/z [M+H]⁺ calcd for $\text{C}_{16}\text{H}_{27}\text{N}_4\text{O}_4$ 339.2027, found 339.2029.

Methyl ((1-Benzyl-1H-1,2,3-Triazol-4-yl)Methyl)-L-Proline (3c)

Compound **3c** was prepared from 45 mg (0.27 mmol) of N-propargyl methyl proline **1**, following the general procedure for the 1,3-dipolar cycloaddition, affording 66 mg of a yellowish oil in 80 % yield. ^1H NMR (300 MHz, CDCl_3): δ 7.42 (s, 1H, C7-H), 7.36–7.30 (m, 3H, Ph), 7.27–7.21 (m, 2H, Ph), 5.48 (d, $J = 2.6$ Hz, 2H, C8-H), 3.95 (d, $J = 13.8$ Hz, 1H, C6-H), 3.78 (d, $J = 13.8$ Hz, 1H, C6-H), 3.60 (s, 3H, OMe), 3.27 (dd, $J = 8.7, 6.1$ Hz, 1H, C2-H), 3.09 (m, 1H, C5-H), 2.48 (dt, $J = 8.4, 8.2$ Hz, 1H, C5-H), 2.18–1.66 (m, 4H, C3-H and C4-H). ^{13}C NMR (75 MHz, CDCl_3): δ 174.6 (COO), 145.1 (C6'), 134.8 (Ph, C), 129.2 (Ph, CH), 128.8 (Ph, CH), 128.3 (Ph, CH), 122.8 (C7), 64.9 (C2), 54.2 (C5), 53.5 (C8), 51.9 (OCH₃), 48.9 (C6), 29.5 (C3), 23.2 (C4). IR (film): ν_{max} 3493, 3140, 2951, 2850, 2359, 1745, 1732, 1556, 1496, 1454, 1359,

1284, 1049, 769, 725 cm^{-1} . ESI-HRMS m/z [M+Na]⁺ calcd for $\text{C}_{16}\text{H}_{20}\text{N}_4\text{NaO}_2$ 323.1478, found 323.1474.

Methyl ((1-Cyclohexyl-1H-1,2,3-Triazol-4-yl)Methyl)-L-Proline (3d)

Compound **3d** was prepared from 45 mg (0.27 mmol) of N-propargyl methyl proline **1**, following the general procedure for the 1,3-dipolar cycloaddition, affording 31 mg of a yellowish oil in 39% yield. ^1H NMR (300 MHz, CDCl_3): δ 7.51 (s, 1H, C7-H), 4.44 (d, $J = 2.6$ Hz, 2H, C8-H), 3.97 (d, $J = 13.8$ Hz, 1H, C6-H), 3.79 (d, $J = 13.8$ Hz, 1H, C6-H), 3.66 (s, 3H, OMe), 3.29 (dd, $J = 8.7, 6.1$ Hz, 1H, C2-H), 3.16–3.10 (m, 1H, C5-H), 2.46 (dt, $J = 8.4, 8.2$ Hz, 1H, C5-H), 2.20–1.63 (m, 12H, C3-H and cyclohexyl), 1.51–1.21 (m, 3H, C4-H and cyclohexyl). ^{13}C NMR (75 MHz, CDCl_3): δ 174.5 (COO), 144.0 (C6'), 120.3 (C7), 64.8 (C2), 59.7 (C5), 53.4 (C8), 51.85 (OCH₃), 48.9 (C6), 33.5 (CH₂), 32.4 (C3), 29.4 (CH₂), 25.2 (CH₂), 23.0 (C4). IR (film): ν_{max} 3417, 3142, 2935, 2856, 2362, 1737, 1732, 1633, 1450, 1371, 1276, 1201, 1049, 997, 894, 823, 777 cm^{-1} . ESI-HRMS m/z [M+H]⁺ calcd for $\text{C}_{15}\text{H}_{25}\text{N}_4\text{O}_2$ 293.1972, found 293.1970.

Methyl ((1-(3-Phenylpropyl)-1H-1,2,3-Triazol-4-yl)Methyl)-L-Proline (3e)

Compound **3e** was prepared from 45 mg (0.27 mmol) of N-propargyl methyl proline **1**, following the general procedure for the 1,3-dipolar cycloaddition, affording 73 mg of a yellowish oil in 82% yield. ^1H NMR (300 MHz, CDCl_3): δ 7.43 (s, 1H, C7-H), 7.24–7.19 (m, 2H, Ph), 7.18–7.08 (m, 3H, Ph), 4.21 (d, $J = 2.6$ Hz, 2H, C8-H), 3.93 (d, $J = 13.8$ Hz, 1H, C6-H), 3.76 (d, $J = 13.8$ Hz, 1H, C6-H), 3.60 (s, 3H, OMe), 3.24 (dd, $J = 8.7, 6.1$ Hz, 1H, C2-H), 3.06 (m, 1H, C5-H), 2.53–2.44 (m, 5H), 2.23–1.61 (m, 4H, C3-H and C4-H). ^{13}C NMR (75 MHz, CDCl_3): δ 174.5 (COO), 144.6 (C6'), 140.3 (Ph), 128.7 (Ph), 128.5 (Ph), 126.4 (Ph), 122.8 (C7), 64.7 (C2), 53.4 (C5), 51.9 (OCH₃), 49.5 (C8), 48.7 (C6), 32.5 (CH₂), 31.7 (C3), 29.5 (CH₂), 23.5 (C4). IR (film): ν_{max} 3626, 3458, 3138, 2949, 2854, 2358, 1732, 1602, 1496, 1444, 1354, 1278, 1172, 1085, 1049, 1004, 785, 748, 702 cm^{-1} . ESI-HRMS m/z [M+Na]⁺ calcd for $\text{C}_{18}\text{H}_{24}\text{N}_4\text{NaO}_2$ 351.1791, found 351.1790.

Methyl ((1-Cinnamyl-1H-1,2,3-Triazol-4-yl)Methyl)-L-Proline (3f)

Compound **3f** was prepared from 45 mg (0.27 mmol) of N-propargyl methyl proline **1**, following the general procedure for the 1,3-dipolar cycloaddition, affording 53 mg of a yellowish oil in 60% yield. ^1H NMR (300 MHz, CDCl_3): δ 7.58 (s, 1H, C7-H), 7.43–7.21 (m, 5H, Ph), 6.65 (d, $J = 15.8$ Hz, 1H, C9-H), 6.33 (m, 1H, C10-H), 5.11 (d, $J = 2.6$ Hz, 2H, C8-H), 4.00 (d, $J = 13.8$ Hz, 1H, C6-H), 3.82 (d, $J = 13.8$ Hz, 1H, C6-H), 3.66 (s, 3H, OMe), 3.31 (dd, $J = 8.7, 6.1$ Hz, 1H, C2-H), 3.14 (m, 1H, C5-H), 2.52 (dt, $J = 8.4, 8.2$ Hz, 1H, C5-H), 2.20–2.04 (m, 1H, C3-H), 2.00–1.71 (m, 3H, C3-H, C4-H₂). ^{13}C NMR (75 MHz, CDCl_3): δ 174.5 (COO), 144.9 (C6'), 135.3 (Ph), 135.3 (C9-H), 128.7 (Ph), 128.5 (CH), 126.7 (Ph), 122.5 (C10-H), 121.9 (C7), 64.7 (C2), 53.4 (C5), 52.3 (OCH₃), 51.8 (C8), 48.7 (C6), 29.4 (C3), 23.0 (C4). IR (film): ν_{max} 3541, 3138, 2951, 2845, 2358, 1741, 1732, 1552,

1448, 1359, 1278, 1203, 1174, 1128, 1047, 970, 756, 694 cm^{-1} . ESI-HRMS m/z $[M+Na]^+$ calcd for $C_{18}H_{22}N_4NaO_2$ 349.1635, found 349.1625.

Methyl ((1-(Naphthalen-2-ylmethyl)-1H-1,2,3-Triazol-4-yl)Methyl)-L-Proline (3g)

Compound **3g** was prepared from 20 mg (0.12 mmol) of N-propargyl methyl proline **1**, following the general procedure for the 1,3-dipolar cycloaddition, affording 34 mg of a light orange solid in 81% yield. M.p. 64.0–64.9 °C. ^1H NMR (300 MHz, CDCl_3): δ 7.85–7.82 (m, 3H, naphthyl), 7.74 (s, 1H, C-H), 7.52–7.49 (m, 2H, naphthyl), 7.46 (s, 1H, C7-H), 7.37–7.33 (m, 1H, naphthyl), 5.66 (d, $J = 3.6$ Hz, 2H, C8-H), 3.97 (d, $J = 13.9$ Hz, 1H, C6-H), 3.80 (d, $J = 13.9$ Hz, 1H, C6-H), 3.60 (s, 3H, OMe), 3.26 (dd, $J = 8.7, 6.1$ Hz, 1H, C2-H), 3.06 (m, 1H, C5-H), 2.46 (dt, $J = 8.4, 8.2$ Hz, 1H, C5-H), 2.15–1.65 (m, 4H, C3-H and C4-H). ^{13}C NMR (75 MHz, CDCl_3): δ 174.4 (COO), 145.1 (C6'), 133.2 (C), 133.1 (C), 131.9 (C), 129.1 (CH), 127.9 (CH), 127.7 (CH), 127.4 (CH), 126.7 (CH), 125.3 (C7), 122.7 (CH), 122.7 (CH), 64.7 (C2), 54.3 (C5), 53.4 (C8), 51.8 (OCH₃), 43.7 (C6), 29.4 (C3), 23.0 (C4). IR (KBr): ν_{max} 3500, 3132, 2949, 2818, 2358, 1732, 1600, 1548, 1508, 1435, 1338, 1273, 1203, 1172, 1126, 1047, 891, 771 cm^{-1} . ESI-HRMS m/z $[M+H]^+$ calcd for $C_{20}H_{23}N_4O_2$ 351.1815, found 351.1826.

Methyl ((1-Octyl-1H-1,2,3-Triazol-4-yl)Methyl)-L-Proline (3h)

Compound **3h** was prepared from 20 mg (0.12 mmol) of N-propargyl methyl proline **1**, following the general procedure for the 1,3-dipolar cycloaddition, affording 31 mg of a yellow oil in 81% yield. ^1H NMR (300 MHz, CDCl_3): δ 7.44 (s, 1H, C7-H), 4.24 (t, $J = 7.2$ Hz, 2H, C8-H), 3.93 (d, $J = 13.8$ Hz, 1H, C6-H), 3.75 (d, $J = 13.8$ Hz, 1H, C6-H), 3.61 (s, 3H, OMe), 3.23 (dd, $J = 8.6, 6.0$ Hz, 1H, C2-H), 3.08–3.02 (m, 1H, C5-H), 2.49–2.41 (dt, 1H, $J = 8.4, 8.1$ Hz, C5-H), 2.03–1.71 (m, 5H), 1.22–1.17 (m, 11H), 0.79 (t, $J = 6.5$ Hz, 3H, CH₃). ^{13}C NMR (75 MHz, CDCl_3): δ 174.4 (COO), 144.4 (C6'), 122.5 (C7), 64.6 (C2), 53.2 (C5), 51.8 (OCH₃), 50.2 (C8), 48.6 (C6), 31.6 (CH₂), 30.2 (CH₂), 29.4 (C3), 29.0 (CH₂), 28.9 (CH₂), 26.4 (CH₂), 23.0 (C4), 22.5 (CH₂), 14.0 (CH₃). IR (film): ν_{max} 3604, 3458, 3136, 2926, 2357, 1345, 1645, 1444, 1354, 1172, 1047, 771 cm^{-1} . ESI-HRMS m/z $[M+Na]^+$ calcd for $C_{17}H_{30}N_4NaO_2$ 345.2261, found 345.2261.

Methyl

((1-Decyl-1H-1,2,3-Triazol-4-yl)Methyl)-L-Proline (3i)

Compound **3i** was prepared from 20 mg (0.12 mmol) of N-propargyl methyl proline **1**, following the general procedure for the 1,3-dipolar cycloaddition, affording 32 mg of a yellow oil in 75% yield. ^1H NMR (300 MHz, CDCl_3): δ 7.49 (s, 1H, C7-H), 4.32 (t, $J = 7.2$ Hz, 2H, C8-H), 4.02 (d, $J = 13.8$ Hz, 1H, C6-H), 3.83 (d, $J = 13.8$ Hz, 1H, C6-H), 3.66 (s, 3H, OMe), 3.33 (dd, $J = 8.7, 6.1$ Hz, 1H, C2-H), 3.17–3.08 (m, 1H, C5-H), 2.58–2.50 (dt, $J = 8.4, 8.2$ Hz, 1H, C5-H), 2.11–1.77 (m, 4H, C3-H and C4-H), 1.27–1.21 (m, 16H), 0.84 (t, $J = 6.6$ Hz, 3H, CH₃). ^{13}C NMR (75 MHz, CDCl_3): δ 174.5 (COO), 144.4 (C6'), 122.7 (C7), 64.7

(C2), 53.4 (C5), 51.9 (OCH₃), 50.4 (C8), 48.7 (C6), 31.9 (CH₂), 30.4 (CH₂), 29.5 (C3), 29.5 (CH₂), 29.3 (CH₂), 29.1 (CH₂), 29.1 (CH₂), 26.5 (CH₂), 23.1 (C4), 22.7 (CH₂), 14.2 (CH₃). IR (film): ν_{max} 3458, 2926, 2854, 2358, 1745, 1732, 1651, 1444, 1373, 1278, 1199, 1172, 1047, 891, 783, 721 cm^{-1} . ESI-HRMS m/z $[M+H]^+$ calcd for $C_{19}H_{35}N_4O_2$ 351.2754, found 351.2746.

Methyl ((1-Hexadecyl-1H-1,2,3-Triazol-4-yl)Methyl)-L-Proline (3j)

Compound **3j** was prepared from 20 mg (0.12 mmol) of N-propargyl methyl proline **1**, following the general procedure for the 1,3-dipolar cycloaddition, affording 22 mg of a white solid in 42% yield. M.p. 60–60.9 °C. ^1H NMR (300 MHz, CDCl_3): δ 7.47 (s, 1H, C7-H), 4.29 (t, $J = 7.2$ Hz, 2H, C8-H), 3.99 (d, $J = 13.8$ Hz, 1H, C6-H), 3.80 (d, $J = 13.8$ Hz, 1H, C6-H), 3.67 (s, 3H, OMe), 3.30 (dd, $J = 8.7, 6.1$ Hz, 1H, C2-H), 3.16–3.11 (m, 1H, C5-H), 2.57–2.48 (dt, $J = 8.9, 7.8$ Hz, 1H, C5-H), 1.91–1.84 (m, 4H), 1.28–1.23 (m, 28H), 0.85 (t, $J = 6.6$ Hz, 3H, CH₃). ^{13}C NMR (75 MHz, CDCl_3): δ 174.7 (COO), 144.7 (C6'), 122.6 (C7), 64.6 (C2), 53.2 (C5), 52.0 (OCH₃), 50.5 (C8), 48.9 (C6), 32.1 (CH₂), 30.5 (CH₂), 29.9 (CH₂), 29.8 (CH₂), 29.8 (CH₂), 29.7 (CH₂), 29.6 (CH₂), 29.6 (CH₂), 29.6 (CH₂), 29.4 (C3), 29.3 (CH₂), 29.2 (CH₂), 28.9 (CH₂), 26.4 (CH₂), 23.0 (C4), 22.6 (CH₂), 14.0 (CH₃). IR (KBr): ν_{max} 3124, 2914, 2357, 1745, 1728, 1556, 1444, 1336, 1269, 1197, 1053, 848, 790, 719 cm^{-1} . ESI-HRMS m/z $[M+Na]^+$ calcd for $C_{25}H_{46}N_4NaO_2$ 457.3513, found 457.3512.

Methyl (Z)-((1-(Octadec-9-en-1-yl)-1H-1,2,3-Triazol-4-yl)Methyl)-L-Proline (3k)

Compound **3k** was prepared from 20 mg (0.12 mmol) of N-propargyl methyl proline **1**, following the general procedure for the 1,3-dipolar cycloaddition, affording 33 mg of a light-yellow oil in 59% yield. ^1H NMR (300 MHz, CDCl_3): δ 7.49 (s, 1H, C7-H), 5.35–5.31 (m, CH=CH, 2H), 4.30 (t, $J = 7.2$ Hz, 2H, C8-H), 4.00 (d, $J = 13.8$ Hz, 1H, C6-H), 3.81 (d, $J = 13.8$ Hz, 1H, C6-H), 3.68 (s, 3H, OMe), 3.30 (dd, $J = 8.8, 6.1$ Hz, 1H, C2-H), 3.15–3.10 (m, 1H, C5-H), 2.56–2.48 (dt, $J = 8.5, 8.1$ Hz, 1H, C5-H), 2.16–1.79 (m, 6H), 1.27–1.25 (m, 26H), 0.87 (t, $J = 6.7$ Hz, 3H, CH₃). ^{13}C NMR (75 MHz, CDCl_3): δ 174.4 (COO), 144.4 (C6'), 130.0 (CH=), 129.7 (CH=), 122.5 (C7), 64.7 (C2), 53.3 (C5), 51.8 (OCH₃), 50.3 (C8), 48.6 (C6), 31.9 (CH₂), 30.3 (CH₂), 29.7 (CH₂), 29.7 (CH₂), 29.5 (C3), 29.4 (CH₂), 29.4 (CH₂), 29.3 (CH₂), 29.1 (CH₂), 29.0 (CH₂), 29.0 (CH₂), 27.2 (CH₂), 27.1 (CH₂), 26.5 (CH₂), 23.0 (C4), 22.6 (CH₂), 14.1 (CH₃). IR (film): ν_{max} 3564, 3477, 3136, 2924, 2852, 2358, 2096, 1745, 1556, 1444, 1373, 1276, 1199, 1172, 1047, 968, 891, 775, 723 cm^{-1} . ESI-HRMS m/z $[M+K]^+$ calcd for $C_{27}H_{48}KN_4O_2$ 499.3408, found 499.3412.

Methyl

((1-Icosyl-1H-1,2,3-Triazol-4-yl)Methyl)-L-Proline (3l)

Compound **3l** was prepared from 20 mg (0.12 mmol) of N-propargyl methyl proline **1**, following the general procedure for the 1,3-dipolar cycloaddition, affording 34 mg of a white solid in 58% yield. M.p. 72.7–73.7 °C. ^1H NMR (300 MHz,

CDCl₃): δ 7.49 (s, 1H, C7-H), 4.31 (t, J = 7.2 Hz, 2H, C8-H), 4.01 (d, J = 13.8 Hz, 1H, C6-H), 3.82 (d, J = 13.8 Hz, 1H, C6-H), 3.69 (s, 3H, OMe), 3.30 (dd, J = 8.5, 5.7 Hz, 1H, C2-H), 3.14–3.1 (m, 1H, C5-H), 2.54–2.46 (dt, J = 8.5, 7.9 Hz, 1H, C5-H), 1.91–1.84 (m, 4H), 1.28–1.23 (m, 36H), 0.87 (t, J = 6.7 Hz, 3H, CH₃). ¹³C NMR (75 MHz, CDCl₃): δ 174.5 (COO), 144.4 (C6'), 122.4 (C7), 64.7 (C2), 53.3 (C5), 51.8 (OMe), 50.2 (C8), 48.6 (CH₂), 31.9 (CH₂), 30.2 (CH₂), 29.6 (CH₂), 29.5 (CH₂), 29.3 (CH₂), 29.0 (CH₂), 26.4 (CH₂), 23.0 (CH₂), 22.6 (CH₂), 14.1 (CH₃). IR (KBr): ν_{\max} 3649, 3124, 3076, 2916, 2846, 2358, 1743, 1462, 1338, 1271, 1211, 1055, 1037, 852, 771, 719 cm⁻¹. ESI-HRMS m/z [M+Na]⁺ calcd for C₂₉H₅₄NaN₄O₂ 513.4139, found 513.4125.

Methyl ((1-(3,7-Dimethylocta-2,6-Dien-1-yl)-1H-1,2,3-Triazol-4-yl)Methyl)-L-Proline (3m)

Compound **3m** was prepared from 30 mg (0.18 mmol) of N-propargyl methyl proline **1**, following the general procedure for the 1,3-dipolar cycloaddition, affording 47 mg of a yellow oil in 87 % yield. ¹H NMR (300 MHz, CDCl₃): δ 7.46 (s, 1H, C7-H), 5.41 (t, J = 7.2 Hz, 1H, C9-H), 5.08–5.01 (m, 1H, C13-H), 4.90 (t, J = 7.2 Hz, 2H, C8-H), 4.01 (d, J = 13.6 Hz, 1H, C6-H), 3.82 (d, J = 13.6 Hz, 1H, C6-H), 3.66 (s, 3H, OMe), 3.30 (dd, J = 8.1, 6.0 Hz, 1H, C2-H), 3.12–3.1 (m, 1H, C5-H), 2.54–2.46 (dt, J = 8.4, 8.2 Hz, 2H, C5-H), 1.7 (m, 6H, C3-H and C4-H), 1.65 (s, 3H, CH₃), 1.63 (m, 6H, CH₃), 1.55 (m, 3H, CH₃). ¹³C NMR (75 MHz, CDCl₃): δ 174.5 (COO), 144.4 (C6'), 122.7 (C7), 64.7 (C2), 53.4 (C5), 51.9 (OCH₃), 50.4 (C8), 48.7 (C6), 31.9 (CH₂), 30.4 (CH₂), 29.5 (C3), 29.3 (CH₂), 29.1 (CH₂), 26.5 (CH₂), 23.1 (C4), 22.7 (CH₂), 17.6 (CH₃), 16.5 (CH₃), 16.0 (CH₃). IR (film): ν_{\max} 3564, 3140, 2926, 2358, 1867, 1747, 1732, 1506, 1435, 1373, 1217, 1174, 1124, 1047, 844, 771 cm⁻¹. ESI-HRMS m/z [M+H]⁺ calcd for C₁₉H₃₅N₄O₂ 351.2754, found 351.2746.

Methyl

((1-((2E,6E)-3,7,11-Trimethyldodeca-2,6,10-Trien-1-yl)-1H-1,2,3-Triazol-4-yl)Methyl)-L-Proline (3n) and Methyl

((1-((2E,6Z)-3,7,11-Trimethyldodeca-2,6,10-Trien-1-yl)-1H-1,2,3-Triazol-4-yl)Methyl)-L-Proline (3o)

Compound **3n** and **3o** were prepared from 50 mg (0.30 mmol) of N-propargyl methyl proline **1**, following the general procedure for the 1,3-dipolar cycloaddition, affording 53 mg of **3n** and 28 mg of **3o** as yellowish oils in 43 % and 23 % yield, respectively.

3n-¹H NMR (300 MHz, CDCl₃): δ 7.47 (s, 1H, C7-H), 5.42 (t, J = 7.2 Hz, 1H, C9-H), 5.08–5.06 (m, 2H, C13-H and C16-H), 4.95 (t, J = 7.2 Hz, 2H, C8-H), 4.00 (d, J = 13.7 Hz, 1H, C6-H), 3.80 (d, J = 13.7 Hz, 1H, C6-H), 3.69 (s, 3H, OMe), 3.31 (dd, J = 8.7, 6.1 Hz, 1H, C2-H), 3.16–3.10 (m, 1H, C5-H), 2.61–2.48 (dt, J = 8.4, 8.2 Hz, 1H, C5-H), 1.70 (m, 4H, C3-H and C4-H), 2.12–1.91 (m, 8H), 1.78 (s, 3H, CH₃), 1.65 (s, 3H, CH₃), 1.63 (m, 3H, CH₃), 1.55 (m, 3H, CH₃). ¹³C NMR (75 MHz, CDCl₃): δ 174.4 (COO), 144.4 (C6'), 143.1 (C), 135.7 (C), 131.3 (C), 124.2 (CH), 123.3 (CH), 122.0 (C7-H), 116.9 (CH), 64.7 (C2), 53.2 (C5), 51.8

(OCH₃), 48.6 (C8), 47.8 (C6), 39.6 (CH₂), 39.4 (CH₂), 29.3 (C3), 26.6 (CH₂), 26.1 (CH₂), 25.6 (CH₂), 22.9 (CH₃), 17.6 (CH₃), 16.5 (CH₃), 16.0 (CH₃). IR (film): ν_{\max} 3417, 3124, 2992, 2358, 1867, 1747, 1732, 1539, 1456, 1317, 1271, 1122, 1047, 773 cm⁻¹. ESI-HRMS m/z [M+H]⁺ calcd for C₂₄H₃₉N₄O₂ 415.3067, found 415.3067.

3o-¹H NMR (300 MHz, CDCl₃): δ 7.47 (s, 1H, C7-H), 5.42 (t, J = 7.2 Hz, 1H, C9-H), 5.08–5.06 (m, 2H, C13-H and C16-H), 4.95 (t, J = 7.2 Hz, 2H, C8-H), 4.00 (d, J = 13.7 Hz, 1H, C6-H), 3.80 (d, J = 13.7 Hz, 1H, C6-H), 3.69 (s, 3H, OMe), 3.31 (dd, J = 8.7, 6.1 Hz, 1H, C2-H), 3.16–3.10 (m, 1H, C5-H), 2.61–2.48 (dt, J = 8.4, 8.2 Hz, 1H, C5-H), 1.7 (m, 4H, C3-H and C4-H), 2.12–1.91 (m, 8H), 1.78 (s, 3H, CH₃), 1.65 (s, 3H, CH₃), 1.63 (m, 3H, CH₃), 1.55 (m, 3H, CH₃). ¹³C NMR (75 MHz, CDCl₃): δ 174.4 (COO), 144.4 (C6'), 143.1 (C), 135.7 (C), 131.3 (C), 124.2 (CH), 123.3 (CH), 122.0 (C7-H), 116.9 (CH), 64.7 (C2), 53.2 (C5), 51.8 (OCH₃), 48.6 (C8), 47.8 (C6), 39.6 (CH₂), 39.4 (CH₂), 29.3 (C3), 26.6 (CH₂), 26.1 (CH₂), 25.6 (CH₂), 22.9 (CH₃), 17.6 (CH₃), 16.5 (CH₃), 16.0 (CH₃). IR (film): ν_{\max} 3417, 3124, 2962, 2924, 2341, 1745, 1732, 1625, 1446, 1435, 1377, 1215, 1172, 1047, 775 cm⁻¹. ESI-HRMS m/z [M+H]⁺ calcd for C₂₄H₃₉N₄O₂ 415.3067, found 415.3067.

Methyl ((1-((E)-3,7,11,15-Tetramethylhexadec-2-en-1-yl)-1H-1,2,3-Triazol-4-yl)Methyl)-L-Proline (3p) and Methyl ((1-(3,7,11,15-Tetramethylhexadec-2-en-1-yl)-1H-1,2,3-Triazol-4-yl)Methyl)-L-Proline (3q)

Compound **3p** and **3q** were prepared from 50 mg (0.30 mmol) of N-propargyl methyl proline **1**, following the general procedure for the 1,3-dipolar cycloaddition, affording 22 mg of **3p** (*E*-isomer) and 23 mg of **3q** (mixture *E:Z*) as yellowish oils in 38 % and 39 % yield, respectively.

3p-¹H NMR (300 MHz, CDCl₃): δ 7.47 (s, 1H, C7-H), 5.39 (t, J = 7.2 Hz, 1H, C9-H), 4.91 (t, J = 7.2 Hz, 2H, C8-H), 3.98 (d, J = 13.7 Hz, 1H, C6-H), 3.78 (d, J = 13.7 Hz, 1H, C6-H), 3.68 (s, 3H, OMe), 3.29 (dd, J = 8.7, 6.1 Hz, 1H, C2-H), 3.14–3.09 (m, 1H, C5-H), 2.54–2.46 (dt, J = 8.4, 8.2 Hz, 1H, C5-H), 2.11 (s, 3H, C10-CH₃), 2.02–1.84 (m, 4H, C3-H and C4-H), 1.77–1.75 (m, 3H), 1.36–1.06 (m, 18H), 0.86–0.81 (m, 12H, CH₃). ¹³C NMR (75 MHz, CDCl₃): δ 174.4 (COO), 144.4 (C6'), 143.7 (C10), 122.1 (C7), 117.4 (C9), 64.8 (C2), 53.7 (C5), 51.9 (OCH₃), 48.7 (C6), 39.8 (C8), 39.4 (CH₂), 37.4 (CH₂), 37.3 (CH₂), 37.0 (CH₂), 36.9 (CH₂), 36.7 (CH₂), 32.7 (CH₂), 32.3 (CH₂), 29.7 (C3), 29.4 (C4), 28.0 (CH₂), 25.5 (CH₂), 25.0 (CH₂), 24.8 (CH₂), 24.5 (CH₃), 23.4 (CH₃), 23.0 (CH₃), 22.7 (CH₃), 22.6 (CH₃). IR (film): ν_{\max} 3500, 3140, 2926, 2358, 1747, 1506, 1456, 1377, 1172, 1047, 933, 862, 775 cm⁻¹. ESI-HRMS: mass calculated for C₂₉H₅₂N₄NaO₂ (M+Na)⁺, 511.3982, found 511.3970.

3q-¹H NMR (300 MHz, CDCl₃): δ 7.47 (s, 1H, C7-H), 5.39 (t, J = 7.2 Hz, 1H, CH), 4.91 (t, J = 7.2 Hz, 2H, C8-H), 3.98 (d, J = 13.7 Hz, 1H, C6-H), 3.78 (d, J = 13.7 Hz, 1H, C6-H), 3.68 (s, 3H, OMe), 3.29 (dd, J = 8.7, 6.1 Hz, 1H, C2-H), 3.14–3.09 (m, 1H, C5-H), 2.54–2.46 (dt, J = 8.4 Hz, J =

8.2 Hz, 1H, C5-H), 2.11 (s, 3H, CH₃), 2.02–1.84 (m, 4H, C3-H and C4-H), 1.77–1.75 (m, 3H), 1.36–1.06 (m, 18H), 0.86–0.81 (m, 12H, CH₃). ¹³C NMR (75 MHz, CDCl₃): δ 174.4 (COO), 144.4 (C6'), 143.7 (C10), 122.1 (C7), 117.4 (C9), 64.8 (C2), 53.7 (C5), 51.9 (OCH₃), 48.7 (C6), 39.8 (C8), 39.4 (CH₂), 37.4 (CH₂), 37.3 (CH₂), 37.0 (CH₂), 36.9 (CH₂), 36.7 (CH₂), 32.7 (CH₂), 32.3 (CH₂), 29.7 (C3), 29.4 (C4), 28.0 (CH₂), 25.5 (CH₂), 25.0 (CH₂), 24.8 (CH₂), 24.5 (CH₃), 23.4 (CH₃), 23.0 (CH₃), 22.7 (CH₃), 22.6 (CH₃). IR (film): ν_{max} 3500, 3140, 2926, 2358, 1747, 1506, 1456, 1377, 1172, 1047, 933, 862, 775 cm⁻¹. ESI-HRMS *m/z* [M+Na]⁺ calcd for C₂₉H₅₂N₄NaO₂ 511.3982, found 511.3970.

BIOLOGY

Reagents

All reagents were purchased from Sigma-Aldrich (St. Louis, MO, USA). Culture medium and fetal calf serum (FCS) were purchased from Cultilab (Campinas, SP, Brazil).

Cells and Parasites

T. cruzi CL strain clone 14 epimastigotes (Brenner and Chiari, 1965) were maintained in the exponential growth phase by subculturing every 48 h in Liver Infusion Tryptose (LIT) medium supplemented with 10% FCS (Vitrocell, Campinas, São Paulo, Brazil) at 28 °C.

Growth Inhibition Assays

T. cruzi epimastigotes in the exponential growth phase (5.0–6.0 × 10⁷ cells mL⁻¹) were cultured in fresh LIT medium. The cells were treated with different concentrations of drugs or not treated (negative control). A combination of Rotenone (60 μM) and Antimycin (0.5 μM) was used as a positive control for inhibition as previously described. (Magdaleno et al., 2009) The cells (2.5 × 10⁶ mL⁻¹) were transferred to 96-well culture plates and incubated at 28 °C. Cell proliferation was quantified by reading the optical density (OD) at 620 nm for 8 days. The OD was converted to cell density values (cells per mL) using a linear regression equation previously obtained under the same conditions. The concentration of compounds that inhibited 50% of parasite proliferation (IC₅₀) was determined during the exponential growth phase (4 days) by fitting the data to a typical sigmoidal dose-response curve using OriginPro8. The compounds were evaluated in quadruplicate in each experiment. The results shown here correspond to three independent experiments. As a cell growth inhibition control, growth curves in which 200 mM rotenone and 0.5 mM antimycin were added to the culture medium were run in parallel for all experiments.

Cytotoxicity Assay

To evaluate the analogs toxicity, Vero cells previously plated on 96 multi-well plate in DMEM 2% FBS and incubated for 48 h at 37 °C in a humid atmosphere containing 5% CO₂, were incubated with 700 μL of DMEM 2% FBS supplemented with each analog for 48 h. The concentration (μM) was different with each analog:

- **3i**: 20 μM, 40 μM, 60 μM, 80 μM, 100 μM and 120 μM.
- **3k**: 5 μM, 10 μM, 15 μM, 20 μM, 25 μM and 30 μM.
- **3n**: 5 μM, 10 μM, 15 μM, 20 μM, 25 μM and 30 μM.
- DMSO: 5 μM, 25 μM, 50 μM and 100 μM.
- Benznidazole: 10 μM, 100 μM, 200 μM and 300 μM.

The viability of cells was measured by MTT dye (3-(4,5-Dimethylthiazol-2-yl)-2,5-diphenyltriazolium bromide, Sigma-Aldrich) colorimetric method. Benznidazole and DMSO were used as positive and negative controls, respectively. Data are expressed as means ± SD of the results of three independent assays of each condition.

L-Proline Transport Inhibition Assay

Parasites in exponential growth phase were washed three times by centrifugation and resuspended in phosphate buffered saline (PBS), pH 7.4. Cells were counted in a Neubauer chamber, adjusted with the same buffer to a final density of 200 × 10⁶ cells/mL and distributed in aliquots of 100 μL (containing 20 × 10⁶ cells each). Transport assays were initiated by the addition to the assay tubes of 100 μL of the desired dilution of L-proline in PBS in the presence of 0.5 mCi of L-[3H] proline. Unless otherwise specified, V₀ was measured at 28 °C for 30 s by incorporation of 0.75 and 3 mM L-proline traced with 1 μCi of U-¹⁴C-L-Pro (Perkin Elmer). In all cases, proline transport was stopped by addition of 800 mL of cold 50 mM proline in PBS (pH 7.4), and rapid washing by centrifugation at 10,000x g for 2 min. Background values in each experiment were measured by simultaneous addition of radiolabeled L-proline and stop solution as previously described (Silber et al., 2002).

Competition Assay

For the competition assays, the transport experiments were performed as described above using the L-Pro concentration corresponding to the *K_m* (0.31 mM). Those conditions were chosen considering an inhibitory activity by structurally related compounds should be competitive, and so, should be evidenced by a change in the *V_{max}* at L-Pro concentrations close to the *K_m*. Non-competitive inhibitors, if any, should diminish *V_{max}*, which is measured at 10 × *K_m* L-Pro (3.1 mM) (Silber et al., 2002).

Statistical Analysis

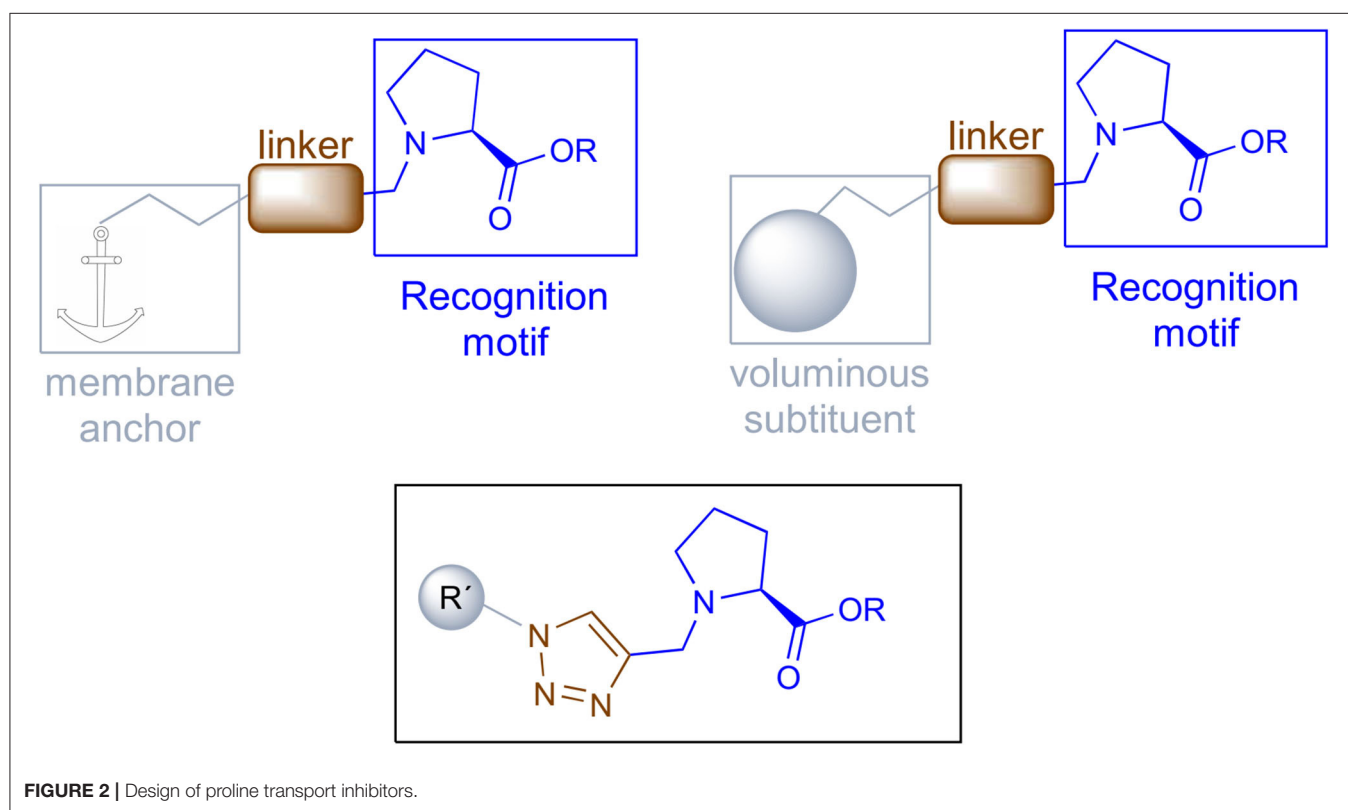
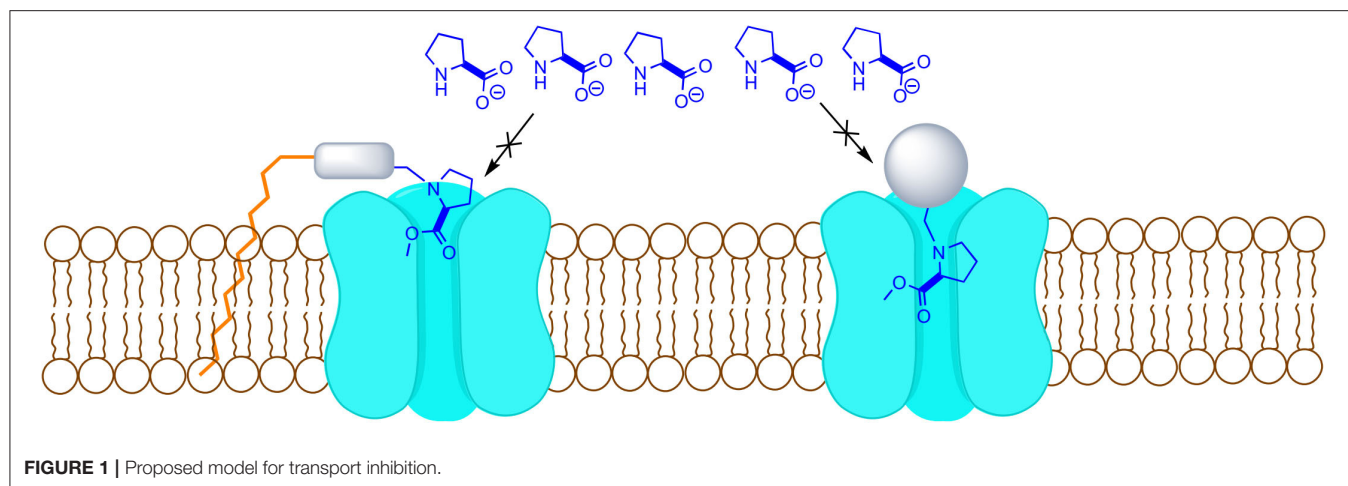
One-way ANOVA followed by the Tukey test was used for statistical analysis. The *T*-test was used to analyze differences between groups. *P* < 0.05 was considered statistically significant.

RESULTS

Synthesis of L-Proline Transport Inhibitors

A proper uptake blocker needs to be recognized by the transporter, but not being able to go through, by adding a bulky substituent or a membrane interacting portion that prevents its transport (**Figure 1**).

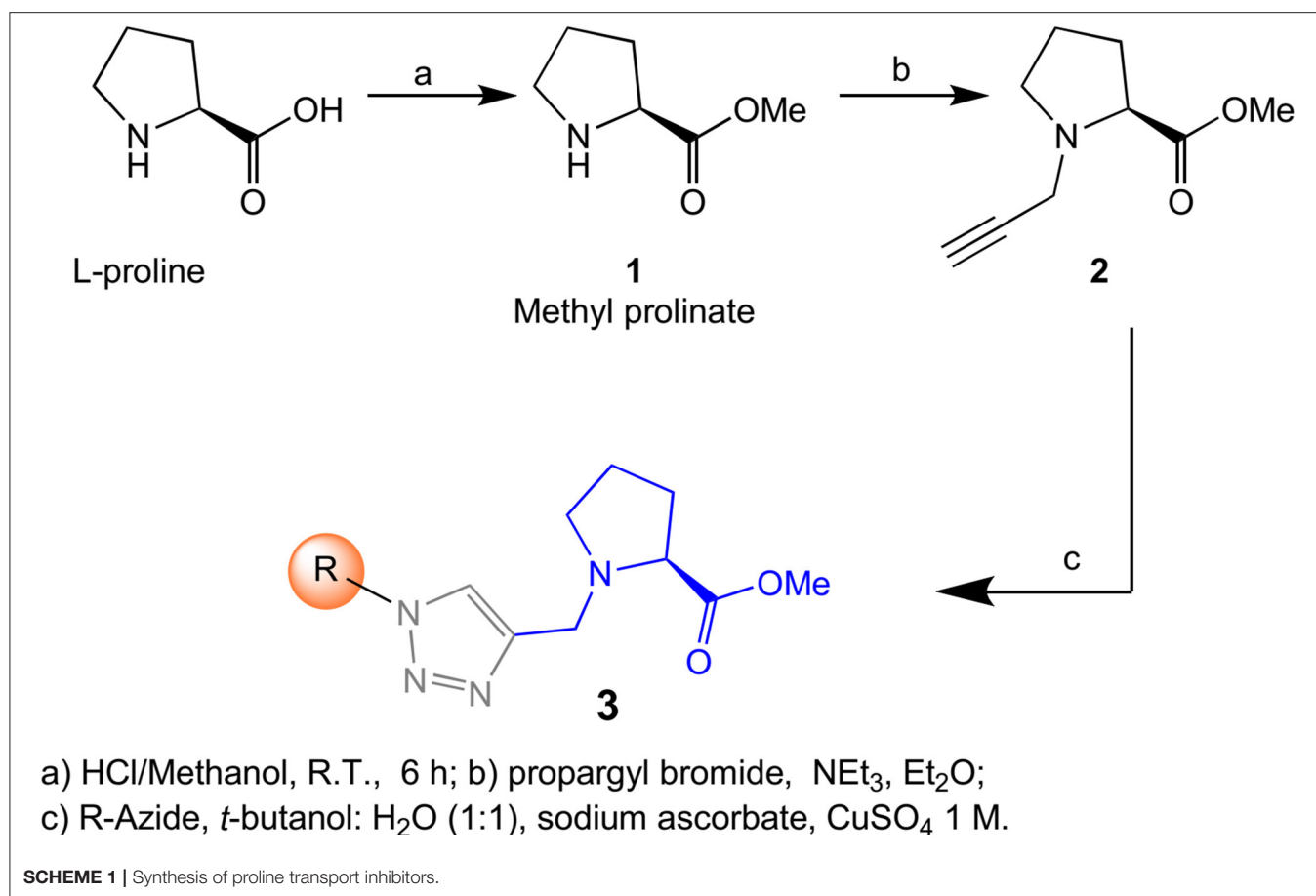
This model will require a compound holding a recognition motif, a linker and a membrane anchor or a voluminous substituent to block the L-proline incorporation. The recognition portion will have L-proline to specifically interact with the



transporter, the membrane anchor should be a non-polar group and both parts will be connected by a 1,2,3-triazole (**Figure 2**).

To validate the proposed model, we proceeded to make a small library following the synthetic strategy shown on **Scheme 1**. The synthesis started from commercial L-proline, preparing the key intermediate in two steps, including an esterification to produce the methyl prolinolate **1** followed by an N-alkylation with propargyl bromide. Once the required key propargyl methyl prolinolate **2** intermediate was prepared, a pool of different azides covering a variety of steric moieties including, aryl, alkyl and isoprenyl substituents was selected to explore their

capacity to interact with the membrane. Azides were prepared by direct substitution of bromide with sodium azide on DMF except for geranyl-, farnesyl-, and phytolazides, which were synthesized from geraniol, farnesol and phytol, respectively, using diphenylphosphorylazide (DPPA) following Thompson's procedure (Thompson et al., 1993). Phytolazide was found to be a mixture of three chemical entities in equilibrium: tertiary azide, *E* and *Z* isomers of the primary azide, following the same behavior previously observed on geranyl-, and farnesylazide (Porta et al., 2014). Allylic azides can be obtained as a mixture, because they exist as equilibrating mixtures of regioisomers due to



the [3,3] sigmatropic rearrangement (Winstein rearrangement) (Gagneuz et al., 1969). That was the case of geranyl, farnesyl and phytolazide, a mixture of primary:tertiary (8:1), being the primary as 1.6:1 (*E:Z*) ratio (Porta et al., 2017b).

Having prepared the pool of azides, we continued with the synthesis of a focused library of inhibitors through click chemistry. Reactions were conducted in a parallel solution synthesis setup under copper (II) sulfate catalytic conditions in water:*t*-BuOH (1:1), using sodium ascorbate as a reductant (Rostovtsev et al., 2002; Labadie et al., 2011; Porta et al., 2017a). In general, reactions needed an excess of azides for completion and a reaction time was 18 h. All the products have 1,4-substitution on the 1,2,3-triazol as expected, based on the original description of this methodology and our previous work (Porta et al., 2014, 2017a). Reactions with aliphatic and benzylic azides produced a single product, with yields that are slightly better for the last ones. The reaction with the mixture of geranyl azides generated **3i**, which was identified as an inseparable mixture of *E* and *Z* isomers (¹H NMR, 1.5:1), in accordance with our previous results (Porta et al., 2017a). When farnesyl azide was used, a mixture of regioisomers was also obtained with the same ratio, but in this case they were separable (Figure 3). When phytolazide was used the same regioisomers were isolated after the reaction with *N*-propargyl methyl proline **1**, presenting a higher *E:Z* ratio (1.8:1). Extensive purification work allowed only the isolation of

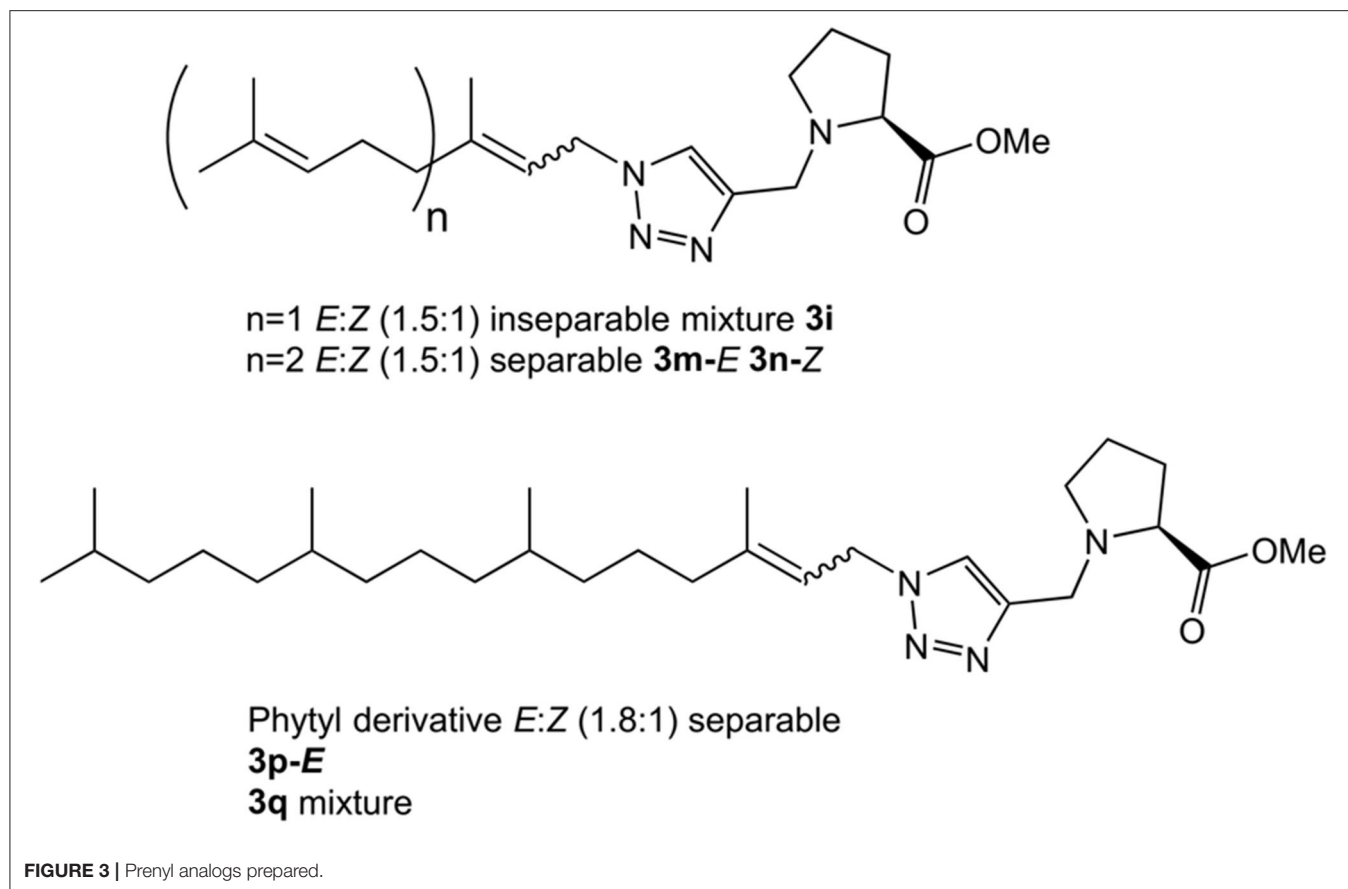
the *E*-isomer of a pure compound (**3p-E**, Figure 3), leaving the remaining product **3q** as a mixture *E:Z*.

Final products **3a-3q**, presented in Table 1, were obtained with an average 67 % yield after purification and were completely characterized by 1D and 2D NMR and ESI-HRMS.

In order to evaluate the biological activity of the prepared collection we decided to initially determine the activity on *T. cruzi* epimastigotes. Then, to validate the L-proline transporter as the molecular target, the intracellular concentration of the amino acid was measured in competition assays with compounds that shown the best antiparasitic activity. Finally, the cytotoxicity of the selected candidates was evaluated in African green monkey kidney epithelial (VERO) cells to estimate the selectivity toward the parasite.

***In vitro* Activity Against *T. cruzi* Epimastigotes**

The compounds collection was assayed against *T. cruzi* epimastigotes (CL strain clone 14) (Brener and Chiari, 1965) at a maximum concentration of 100 μM. Eight compounds of the total list did not affect the parasite growth at that concentration (**3a**, **3b**, **3c**, **3d**, **3e**, **3f**, **3h**, **3m**), being considered inactive. (Table 1) The naphthyl derivative **3g** and the eicosanyl analog **3l** have an IC₅₀ of 100 μM. A second group of active members of the collection includes the remaining prenyl derivatives **3n**, **3o**,



3p and **3p** with IC_{50} s 48.32, 58.60, 69.75, 48.27 μM , respectively. (Table 1) The remaining group contains the aliphatic derivatives **3i**, **3j** and **3k**. Those compounds have IC_{50} s below 40 μM , being the most active members the collection. The decyl and the oleyl derivatives **3i** and **3k** have similar activity (IC_{50} of 38.97 and 35.06 μM , respectively), while the cetyl analog **3j** has a IC_{50} of 24.07 μM , considerably slower than the other two (Table 1).

In vitro Cytotoxicity Assay on Vero Cells

Vero cells are well established model to test cytotoxicity *in vitro* because it is an aneuploid and a continuous cell lineage. Initially the library was screened at a fix concentration of 4.75 $\mu\text{g}/\text{mL}$ and none of the analogs showed cytotoxic activity. The most active analogs of the series, compounds **3i**, **3j**, **3k**, and **3n**, were submitted to a further analysis to determine their IC_{50} . Compound **3j** was not soluble at 50 μM which made not possible to calculate its IC_{50} . Analogs **3i**, **3k**, and **3n** were soluble in a concentration range allowing to perform the assay, showing IC_{50} of 43 μM , 17 μM and 14 μM , respectively.

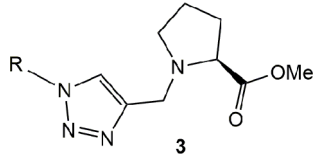
Proline Transport Assay

In order to obtain a deeper insight into the molecular mechanism of the most active compounds, we performed a proline transport competition assay. The compounds with an IC_{50} lower than 50 μM (**3i**, **3j**, **3k**, and **3n**) were selected to perform the proline uptake assay aiming to determine the transport inhibition

(Magdaleno et al., 2009). The analogs were assayed on *T. cruzi* epimastigotes incubated with proline at the transporter K_m concentration (0.31 mM), and the analogs were assayed at concentration 10-fold higher (3.1 mM). Surprisingly, we observed that the compounds with higher activity on *T. cruzi* epimastigotes (lower IC_{50} values) showed inhibition but they were not strong enough when compared to analogs with lower antiparasitic activity (higher IC_{50} values). As can be seen on Figure 4, compounds **3i** (*T. cruzi* epimastigotes IC_{50} = 38 μM) and **3n** (*T. cruzi* epimastigotes IC_{50} = 49 μM) showed a proline transport inhibition higher than 75% being more active than the analog **3j** that only produced an inhibition of 20%. The oleyl derivate (**3k**), with an unsaturated fatty tail, has a similar IC_{50} on *T. cruzi* epimastigotes compared to the cetyl analog (**3j**) showing no inhibition in terms of proline uptake (Table 2).

DISCUSSION

The selective inhibition of transporters has been proposed as a valuable target to develop new medications against different pathologies including neurological disorders (Qosa et al., 2016) and parasitic diseases (Sayé et al., 2019). The specific inhibition of neuronal glycine, alanine, serine, and cysteine transporters have been studied as molecular targets for new treatment of schizophrenia (Pinard et al., 2010; Schneider et al., 2012;

TABLE 1 | Anti-*T. cruzi* activity of the proline derivatives.


Compound	R	Yield (%)	<i>T. cruzi</i> ^a IC ₅₀ [μM]
3a	CH ₂ COOEt	80	>100
3b	(CH ₂) ₄ COOEt	69	>100
3c	Bn	80	>100
3d	Cyclohexyl	39	>100
3e	Ph-CH ₂ CH ₂ CH ₂	82	>100
3f	Cinnamyl	60	>100
3g	CH ₂ -naphthyl	81	100
3h	Octyl	81	>100
3i	Decyl	75	38.97 ± 1.37
3j	Cetyl	42	24.07 ± 0.66
3k	Oleyl	59	35.06 ± 6.96
3l	Eicosanyl	58	100
3m	Geranyl	87	>100
3n	<i>E</i> -Farnesyl	43	48.32 ± 1.29
3o	<i>Z</i> -Farnesyl	23	58.60 ± 1.37
3p	<i>E</i> -Phytyl	38	69.75 ± 2.17
3q	Phytyl-Mixture	39	48.27 ± 5.81
Benznidazole			7.00 [57]

^aEpimastigotes CL14, results shown are means (SD) from the three independent experiments.

Carland et al., 2014). A high-affinity transporter for proline has been identified, providing an important evidence for proline as a neurotransmitter (Hauptmann et al., 1983). A high throughput screening campaign for high affinity proline transporter inhibitors resulted in the identification of the selective inhibitor LP-403812 (Yu et al., 2009). Summarizing, the participation of metabolites uptake in critical processes in health and diseases has been well demonstrated.

A systematic design pipeline for molecules targeting molecular transporters has not been properly explored. The discovery of most of transporters inhibitors happened by chance or through large HTS campaigns. Burns et al. (2009) pioneered a work in this sense proposing a polyamine-fatty acid conjugate as a polyamine transporter inhibitor. In their rational, the polyamine portion is recognized by the transporter and the fatty acid interacts with the membrane, blocking the polyamine entrance. The newly designed inhibitors (L-Lyz(C18-Acyl-spermine) combined with DMFO display selective antitumoral activity. All the inhibitors mentioned before contained an amino acid portion, or an amino acid mimic, that is recognized by the transporter as a common feature (Figure 5).

With those precedents in mind, we proposed/presented here a general model for aminoacid transporter inhibitors. Our model

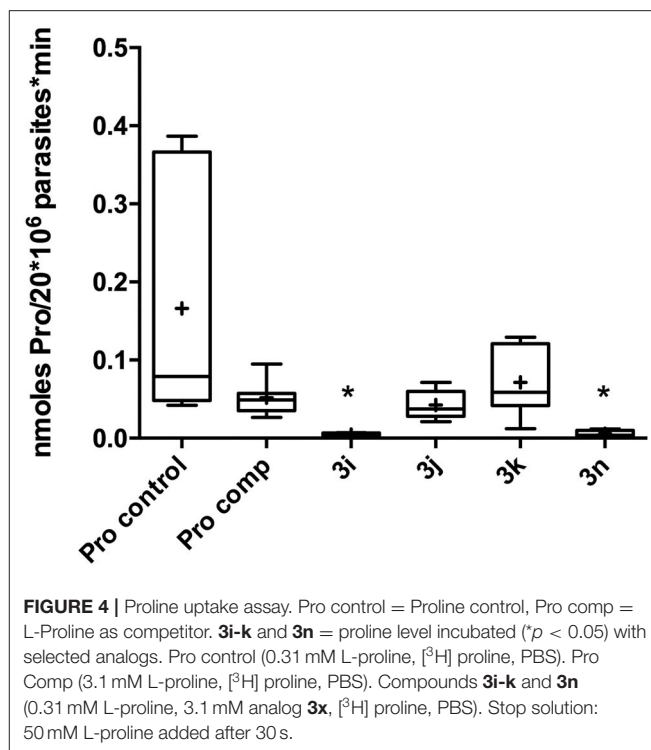


FIGURE 4 | Proline uptake assay. Pro control = Proline control, Pro comp = L-Proline as competitor. **3i-k** and **3n** = proline level incubated (**p* < 0.05) with selected analogs. Pro control (0.31 mM L-proline, [³H] proline, PBS). Pro Comp (3.1 mM L-proline, [³H] proline, PBS). Compounds **3i-k** and **3n** (0.31 mM L-proline, 3.1 mM analog **3x**, [³H] proline, PBS). Stop solution: 50 mM L-proline added after 30 s.

TABLE 2 | Proline uptake inhibition of selected analogs.

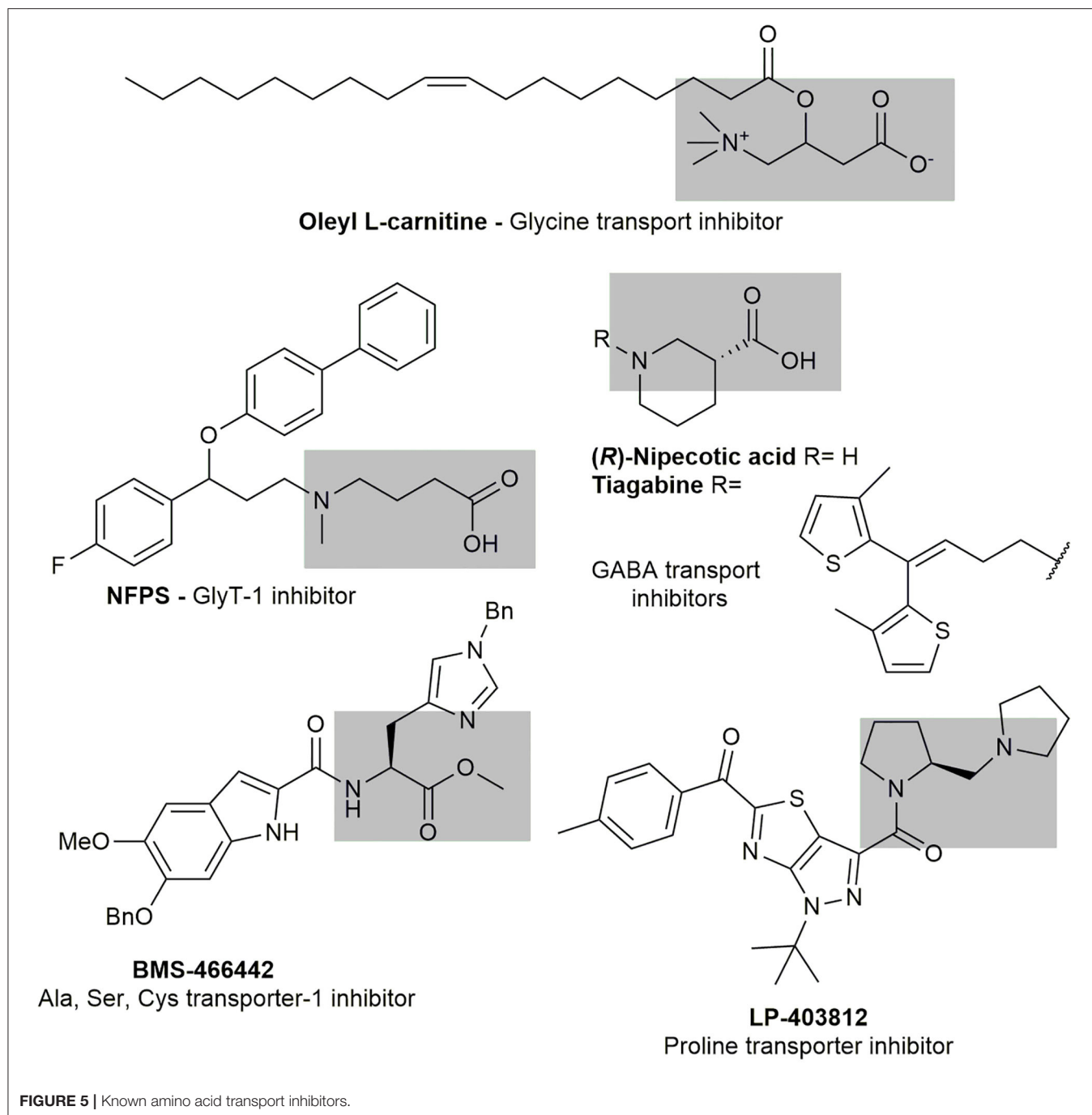
Compound	R	<i>T. cruzi</i> IC ₅₀ [μM]	% of Proline inh.
3i	Decyl	38.97 ± 1.37	87
3j	Cetyl	24.07 ± 0.66	18 [#]
3k	Oleyl	35.06 ± 6.96	0
3n	<i>E</i> -Farnesyl	48.32 ± 1.29	99

[#]Precipitation was observed over the experiment.

included an aminoacid portion for recognition, linked to a variable region with different lipophilic and bulk substituents.

We identified the 1,2,3-triazole as a proper linker for our transport inhibitors. The neutral nature of this heterocycle has properly suited the requirements for bioconjugation, protein labeling and immobilization (Gauchet et al., 2006; McKay and Finn, 2014) and for combining different pharmacophores to make hybrid compounds or chimeras. The Cu(I) azide-alkyne reaction, the quintessence of click chemistry, had a strong impact in many research areas including Medicinal Chemistry (Tron et al., 2008; Agalave et al., 2011). The easy reaction conditions has made this methodology very useful to rapidly prepare libraries of compounds, including antiparasitic drug candidates (Carvalho et al., 2010; Hamann et al., 2014; Porta et al., 2017a).

Using 1,2,3-triazole as linker, we prepared products introducing substituents with proper membrane anchor properties. Fatty acids and isoprenyl chains are selectively introduced in proteins by post translational modifications and served as a mediator for membrane association increasing



their molecular hydrophobicity (Hannoush and Sun, 2010). Looking to produce similar anchoring properties, isoprenyl and linear long alkyl chain were selected as some of the 1,2,3-triazole substituents, introduced as azide on the heterocycle. Additionally, azides with bulky substituent were also used looking to obstruct the transporter. A library of 17 compounds was finally prepared including two alkyl ester, five alicyclic and aryl, five alkyl and five prenyl derivatives.

The proline uptake systems have similar biochemical characteristics in epimastigotes and the mammalian *T. cruzi*

stages (Silber et al., 2002; Tonelli et al., 2004). It has been demonstrated that these stages are sensitive to proline availability (Tonelli et al., 2004) and uptake (Magdaleno et al., 2009). With those precedents in mind, we decided to evaluate the activity on epimastigotes. The results of the inhibition on *T. cruzi* epimastigotes shown that half of the compounds prepared did not show activity at the maximum concentration tested of 100 μ M. Between the inactive analogs, **3a** and **3b** holds the shortest substituents of the library and have esters on the side-chain. Being the most polar substituent of the series and

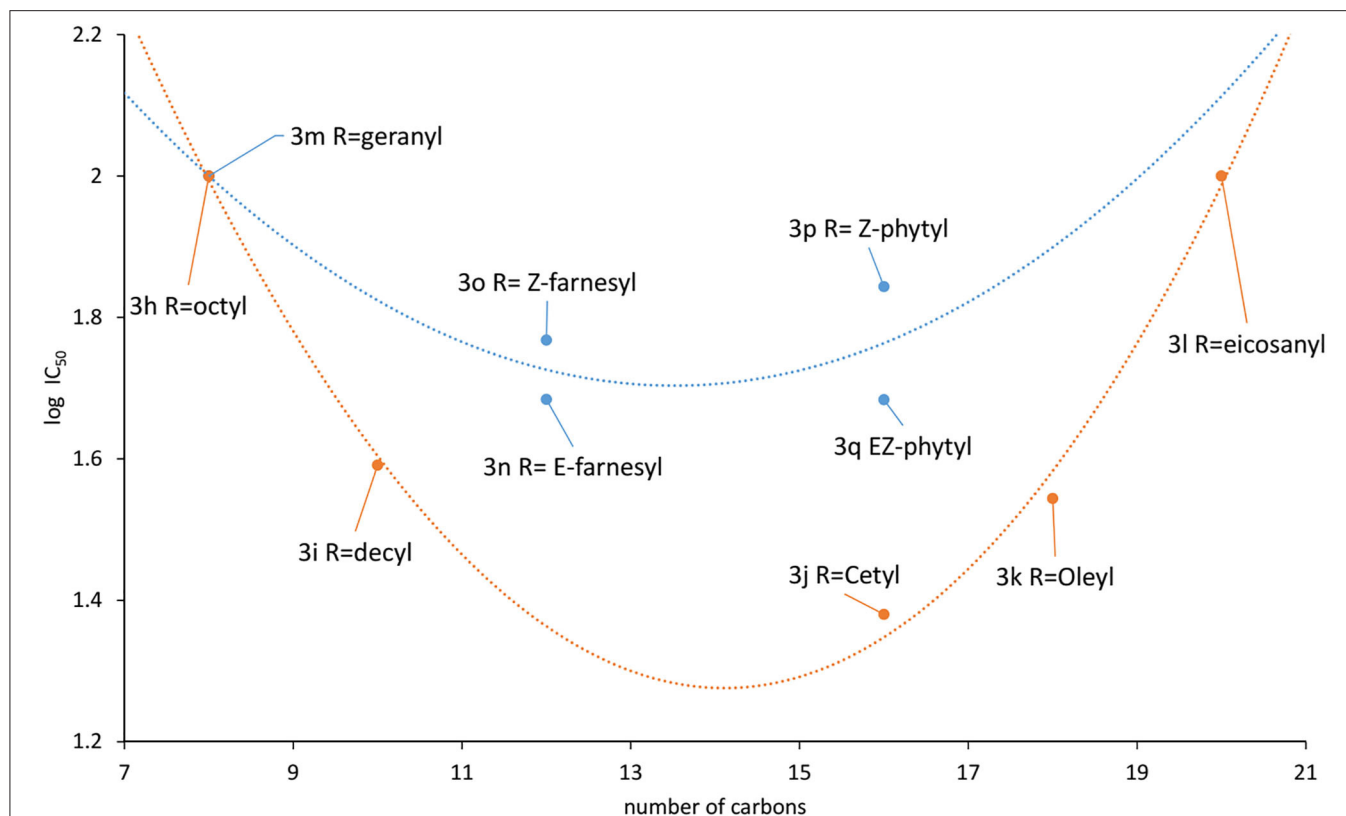


FIGURE 6 | Correlation between activity and substituents chain length (blue: prenyl, orange: aliphatic).

susceptible to hydrolysis, seems to be a possible explanation for the lack of activity. Analogs **3c**, **3d**, **3e**, and **3f**, contain non-polar cyclic substituents either aryl or alicyclic, were also inactive. Interestingly, the naphthyl derivative **3g**, the bulkier member of the collection, has an IC_{50} of $100 \mu M$. Together those results shown that polycyclic bulky substituents could be required to improve the activity. Nevertheless, the fact that the aromatic analogs were inactive discouraged the idea that π -stacking interactions are involved on the binding to the molecular target.

As was mentioned before, fatty acids and isoprenyl chains contribute as mediators for protein membrane anchoring, therefore, ten analogs were included with those substituents. The hypothesis that this kind of substituents contribute to improve the activity, seems to be validated because only the analogs holding the shorter substituents, **3h** (R=octyl) and **3m** (R=geranyl) were inactive. A detailed look at the aliphatic derivatives' activities did not show a direct correlation between the IC_{50} and the chain length. The activity increases from octyl **3i** to decyl **3h** derivative ($IC_{50} > 100$ and 38.27 mM, respectively), being the cetyl analog **3j**, the most active (IC_{50} 24.54 mM). Then, the activity decreases to 35.06 mM for the oleyl derivative **3k** and 100 mM for the eicosanyl analog **3l**. A similar behavior is observed for the prenyl derivatives, but in this case the difference is less pronounced. Moving from the geranyl derivative **3h** to the farnesyl analogs the activity increase to 48.32 mM for the *E*-isomer **3n** that is slightly more active than the *Z*-isomer **3o** (59.60 mM). Then, as happened with the alkylated analogs, the

activity decreases for the longer member of the family, the phytyl derivatives **3p** (*E*-isomer) and **3q** (*E/Z* mixture), with IC_{50} s 69.75 and 48.27 mM, respectively.

A tendency can be visualized when the $\log IC_{50}$ was plotted against the carbon chain length and the aliphatic and the prenylated are separately correlated (Figure 6). One interesting outcome of this chart is that both curves have their minimum around 14 carbon atoms, that appears to be the optimal chain length for the activity.

These comparisons of the compounds have shown that most of them are considerable more active than L-thiazolidine-4-carboxylic acid (T4C), the only reported antichagasic proline derivative, with an IC_{50} of $890 \mu M$ on *T. cruzi* epimastigotes (Magdaleno et al., 2009). Analogs **3j**, **3i**, **3k**, **3n** were 36, 23, 22, and 18 times more active than T4C. That marked difference on the activity highlight the importance of the proline ring decoration on the antiparasitic activity.

The cytotoxicity of most active compounds (analogs **3i**, **3k**, and **3n**) were tested in cultured monkey kidney Vero cells to estimate the selectivity toward the parasite. The IC_{50} were $43 \mu M$, $17 \mu M$ and $14 \mu M$, respectively, being an adequate concentration window for future studies in intracellular stages. The selectivity index, (calculated as IC_{50} Vero cells / IC_{50} *T. cruzi* epimastigotes) were 1.13, 0.43 and 0.25 for compounds **3i**, **3k**, and **3n**, respectively. This numbers shown a similar susceptibility to the mentioned compounds. The toxicity displayed may be linked to the proline transport inhibition, but that hypothesis must be

validated. These results are not promising at this point to propose that compounds of our collection could be good candidates for anti-chagasic drug development. Nevertheless, the applied strategy settles the basis to design inhibitors against *T. cruzi* biological targets in both, the insect, and the mammalian stages.

Finally, to validate the L-proline transporter as the molecular target, the intracellular concentration of the amino acid was measured in competition assays with compounds that shown the best antiparasitic activity. Analogs **3i**, **3k**, and **3n** were assayed. Interestingly, the proline uptake inhibition of those compounds did not follow the antiparasitic activity. The first hypothesis to explain that behavior was based on the presence of unsaturations on fatty tail. The difference between **3i** and **3k** relay on the unsaturation on the oleyl chain of the last. The structure of **3k** shows a twisted conformation produced by the C9-double bond that also restricts the rotation around the neighbor bonds. Furthermore, the tail length of **3i** and **3k** differ in 6 carbon and the most active is the decyl analog (**3i**) in terms of transport inhibition, matching the behavior displayed in **Figure 6**. The *E*-farnesyl derivative **3n** has a trimethyl substituted side-chain that is twelve carbon long, with three double bonds. Interestingly, this analog produced a complete inhibition of the proline uptake but is the less active of this series against *T. cruzi*. (**Table 2**) The fact that this analog was a superior inhibitor of the transporter could be the result of a better binding. Also, it could be attributed to the markedly different conformation of the analog due to the restricted rotation of the isoprenyl chain. Those restrictions should contribute to block the transporter once the proline region is recognized (Sayé et al., 2017). The inhibition of proline uptake by analogs **3i** and **3n**, resulted considerably more active than that inhibition by T4C (Magdaleno et al., 2009). Those differences were clearly related with the N1-allylated-1,2,3-triazolyl chain introduced on the proline.

CONCLUSIONS

In the present study, a strategy to design amino acids transport inhibitors was proposed. The uptake blocker is composed by a recognition motif, a linker and a bulky substituent or a membrane interacting portion. A set of seventeen 1,5-substituted-1,2,3-triazole derivatives of methyl proline were prepared to validate the design. They were initially assayed against *T. cruzi* epimastigotes showing comparable potency than the control drug benznidazole. The antiparasitic activity profile of the series allowed us to establish a well-defined structural-activity relationship were the nature of the side-chain play a critical role. In order to validate the design, the inhibition of the proline uptake was studied with the analogs **3i**, **3j**, **3k**, and **3n** that displayed the best antiparasitic activity. The analogs with **3i** (R=decyl) and **3n** (R=*E*-farnesyl) produced a markedly reduction of the internalized proline. Those studies are strong evidence to validate our design of the transporter inhibitor that also linked the antiparasitic activity with the proline uptake.

The proline uptake has been explored as target for Chagas disease by drug repurposing. Using that approach, crystal violet has been identified as an interesting candidate (Sayé et al., 2020).

Our approach is the first report of new compounds that have been design, prepared and validated as proline uptake blockers with antiparasitic activity. Unfortunately, the most active products displayed low selectivity toward the parasite, not being good candidates for future development as antichagasic drugs. Nevertheless, a complete study on the other *T. cruzi* life cycle stages could confirm or discard that hypothesis. The validated design of aminoacid transport inhibitor should open new applications on the study of physiological role of amino acid transporters in the central nervous system.

DATA AVAILABILITY STATEMENT

The raw data supporting the conclusions of this article will be made available by the authors, without undue reservation.

AUTHOR CONTRIBUTIONS

LF and EP-Z were responsible for the synthesis, purification and structural characterization of all the products. LF and MB performed the antiproliferative assays against *Trypanosoma cruzi*, carried out the proline transport inhibition assays, and interpreted the results. LF and LP performed the cytotoxicity assays on Vero cells. GL wrote most of the manuscript and supervised the study. GL, AS, and JC were the project leaders organizing and guiding experiments. All authors contributed to refining the manuscript and approved the final manuscript.

FUNDING

The authors wish to express their gratitude to UNR (Universidad Nacional de Rosario, Bio503), Agencia Nacional de Promoción Científica y Tecnológica (ANPCyT PICT- 2017-2096 awarded to GL) and Fundação de Amparo à Pesquisa do Estado de São Paulo grants 2016/06034-2 (awarded to AS) and Conselho Nacional de Pesquisas Científicas e Tecnológicas (CNPq) grants 404769/2018-7 and 308351/2013-4 (awarded to AS). The research leading to these results has, in part, received funding from the UK Research and Innovation via the Global Challenges Research Fund under grant agreement A Global Network for Neglected Tropical Diseases grant number MR/P027989/1. GL and JC are members of the Research Career of the Consejo Nacional de Investigaciones Científicas y Técnicas of Argentina (CONICET). LF, EP-Z, and LP thanks CONICET for the award of a Fellowship.

ACKNOWLEDGMENTS

This manuscript has been released as a pre-print at ChemRxiv (Fargnoli et al., 2019).

SUPPLEMENTARY MATERIAL

The Supplementary Material for this article can be found online at: <https://www.frontiersin.org/articles/10.3389/fchem.2020.00696/full#supplementary-material>

REFERENCES

- Agalave, S. G., Maujan, S. R., and Pore, V. S. (2011). Click Chemistry: 1,2,3-Triazoles as Pharmacophores. *Chem. Asian J.* 6, 2696–2718. doi: 10.1002/asia.201100432
- Avila, C. C., Mule, S. N., Rosa-Fernandes, L., Viner, R., Barison, M. J., Costa-Martins, A. G., et al. (2018). Proteome-wide analysis of *Trypanosoma cruzi* exponential and stationary growth phases reveals a subcellular compartment-specific regulation. *Genes* 9:413. doi: 10.3390/genes9080413
- Barison, M. J., Damasceno, F. S., Mantilla, B. S., and Silber, A. M. (2016). The active transport of histidine and its role in ATP production in *Trypanosoma cruzi*. *J. Bioenerg. Biomembr.* 48, 437–449. doi: 10.1007/s10863-016-9665-9
- Barisón, M. J., Rapado, L. N., Merino, E. F., Pral, E. M. F., Mantilla, B. S., Marchese, L., et al. (2017). Metabolomics profiling reveals a finely tuned, starvation-induced metabolic switch in *Trypanosoma cruzi* epimastigotes. *J. Biol. Chem.* 292, 8964–8977. doi: 10.1074/jbc.M117.778522
- Brener, Z., and Chiari, E. (1965). Aspects of early growth of different *Trypanosoma cruzi* strains in culture medium. *J. Parasitol.* 51, 922–926. doi: 10.2307/3275869
- Burns, M. R., Graminski, G. F., Weeks, R. S., Chen, Y., and O'Brien, T. G. (2009). Lipophilic lysine–spermine conjugates are potent polyamine transport inhibitors for use in combination with a polyamine biosynthesis inhibitor. *J. Med. Chem.* 52, 1983–1993. doi: 10.1021/jm801580w
- Carland, J. E., Handford, C. A., Ryan, R. M., and Vandenberg, R. J. (2014). Lipid inhibitors of high affinity glycine transporters: Identification of a novel class of analgesics. *Neurochem. Int.* 73, 211–216. doi: 10.1016/j.neuint.2013.08.012
- Carvalho, I., Andrade, P., Campo, V. L., Guedes, P. M., Sesti-Costa, R., Silva, J. S., et al. (2010). ‘Click chemistry’ synthesis of a library of 1,2,3-triazole-substituted galactose derivatives and their evaluation against *Trypanosoma cruzi* and its cell surface trans-sialidase. *Bioorg. Med. Chem.* 18, 2412–2427. doi: 10.1016/j.bmc.2010.02.053
- Contreras Vt, A.-J. T., Bonaldo, M. C., Thomaz, N., Barbosa, H. S., Meirelles Mde, N., and Goldenberg, S. (1988). Biological aspects of the Dm 28c clone of *Trypanosoma cruzi* after metacyclogenesis in chemically defined media. *Mem. Inst. Oswaldo Cruz.* 83, 123–133. doi: 10.1590/S0074-02761988000100016
- Crispim, M., Damasceno, F. S., Hernández, A., Barisón, M. J., Pretto Sauter, I., Souza Pavani, R., et al. (2018). The glutamine synthetase of *Trypanosoma cruzi* is required for its resistance to ammonium accumulation and evasion of the parasitophorous vacuole during host-cell infection. *PLoS Negl. Trop. Dis.* 12:e0006170. doi: 10.1371/journal.pntd.0006170
- Fargnoli, L., Panozzo-Zéner, E. A., Pagura, L., Barisón, M. J., Cricco, J. A., Silber, A. M., et al. (2019). New L-proline uptake inhibitors with anti-*Trypanosoma cruzi* activity. *ChemRxiv*. doi: 10.26434/chemrxiv.7564991. [Epub ahead of print].
- Gagneuz, A., Winstein, S., and Young, W. G. (1969). Rearrangement of allyl azides. *J. Org. Chem.* 1, 5956–5957. doi: 10.1021/ja01507a045
- Gauchet, C., Labadie, G. R., and Poulter, C. D. (2006). Regio- and chemoselective covalent immobilization of proteins through unnatural amino acids. *J. Am. Chem. Soc.* 128, 9274–9275. doi: 10.1021/ja061131o
- Girard, R. M. B. M., Crispim, M., Alencar, M. B., and Silber, A. M. (2018). Uptake of L-Alanine and Its Distinct Roles in the Bioenergetics of *Trypanosoma cruzi*. *mSphere* 3, e00338–e00338. doi: 10.1128/mSphereDirect.00338-18
- Guedes, P. M. M., Silva, G. K., Gutierrez, F. R. S., and Silva, J. S. (2011). Current status of Chagas disease chemotherapy. *Expert Rev. Anti Infect. Ther.* 9, 609–620. doi: 10.1586/eri.11.31
- Hamann, A. R., De Kock, C., Smith, P. J., Van Otterlo, W. A., and Blackie, M. A. (2014). Synthesis of novel triazole-linked mefloquine derivatives: biological evaluation against *Plasmodium falciparum*. *Bioorg. Med. Chem. Lett.* 24, 5466–5469. doi: 10.1016/j.bmcl.2014.10.015
- Hannoush, R. N., and Sun, J. (2010). The chemical toolbox for monitoring protein fatty acylation and prenylation. *Nat. Chem. Biol.* 6, 498–506. doi: 10.1038/nchembio.388
- Hauptmann, M., Wilson, D. F., and Erecinska, M. (1983). High affinity proline uptake in rat brain synaptosomes. *FEBS Lett.* 161, 301–305. doi: 10.1016/0014-5793(83)81029-1
- Labadie, G. R., De La Iglesia, A., and Morbidoni, H. R. (2011). Targeting tuberculosis through a small focused library of 1,2,3-triazoles. *Mol. Divers.* 15, 1017–1024. doi: 10.1007/s11030-011-9319-0
- Magdaleno, A., Ahn, I. Y., Paes, L. S., and Silber, A. M. (2009). Actions of a proline analogue, L-thiazolidine-4-carboxylic acid (T4C), on *Trypanosoma cruzi*. *PLoS ONE* 4:e4534. doi: 10.1371/journal.pone.0004534
- Mantilla, B. S., Marchese, L., Casas-Sánchez, A., Dyer, N. A., Ejeh, N., Biran, M., et al. (2017). Proline metabolism is essential for *trypanosoma brucei* survival in the tsetse vector. *PLoS Path.* 13:e1006158. doi: 10.1371/journal.ppat.1006158
- Mantilla, B. S., Paes, L. S., Pral, E. M. F., Martil, D. E., Thiemann, O. H., Fernández-Silva, P., et al. (2015). Role of Δ 1-Pyrroline-5-carboxylate dehydrogenase supports mitochondrial metabolism and host-cell invasion of *Trypanosoma cruzi*. *J. Biol. Chem.* 290, 7767–7790. doi: 10.1074/jbc.M114.574525
- Marchese, L., Nascimento, J., Damasceno, F., Bringaud, F., Michels, P., and Silber, A. (2018). The uptake and metabolism of amino acids, and their unique role in the biology of pathogenic trypanosomatids. *Pathogens* 7:36. doi: 10.3390/pathogens7020036
- Martins, R. M., Covarrubias, C., Rojas, R. G., Silber, A. M., and Yoshida, N. (2009). Use of L-proline and ATP production by *Trypanosoma cruzi* metacyclic forms as requirements for host cell invasion. *Infect. Immun.* 77, 3023–3032. doi: 10.1128/IAI.00138-09
- Mckay, C. S., and Finn, M. G. (2014). Click chemistry in complex mixtures: bioorthogonal bioconjugation. *Chem. Biol.* 21, 1075–1101. doi: 10.1016/j.chembiol.2014.09.002
- Morillo, C. A., Marin-Neto, J. A., Avezum, A., Sosa-Estani, S., Rassi, A. Jr., Rosas, F., et al. (2015). Randomized trial of benznidazole for chronic chagas’ cardiomyopathy. *New Engl. J. Med.* 373, 1295–1306. doi: 10.1056/NEJMoa1507574
- Nunes, M. C. P., Dones, W., Morillo, C. A., Encina, J. J., and Ribeiro, A. L. (2013). Chagas disease: an overview of clinical and epidemiological aspects. *J. Am. Coll. Cardiol.* 62, 767–776. doi: 10.1016/j.jacc.2013.05.046
- Paes, L. S., Suárez Mantilla, B., Zimbres, F. M., Pral, E. M. F., Diogo De Melo, P., Tahara, E. B., et al. (2013). Proline dehydrogenase regulates redox state and respiratory metabolism in *Trypanosoma cruzi*. *PLoS ONE* 8:e69419. doi: 10.1371/journal.pone.0069419
- Pereira, C. A., Alonso, G. D., Paveto, M. C., Iribarren, A., Cabanas, M. L., Torres, H. N., et al. (2000). *Trypanosoma cruzi* arginine kinase characterization and cloning: a novel energetic pathway in protozoan parasites. *J. Biol. Chem.* 275, 1495–1501. doi: 10.1074/jbc.275.2.1495
- Pérez-Molina, J. A., and Molina, I. (2018). Chagas disease. *Lancet* 391, 82–94. doi: 10.1016/S0140-6736(17)31612-4
- Pinard, E., Alanin, A., Alberati, D., Bender, M., Borroni, E., Bourdeaux, P., et al. (2010). Selective GlyT1 inhibitors: discovery of [4-(3-Fluoro-5-trifluoromethylpyridin-2-yl)piperazin-1-yl][5-methanesulfonyl-2-((S)-2,2,2-trifluoro-1-methylethoxy)phenyl]methanone (RG1678), a promising novel medicine to treat schizophrenia. *J. Med. Chem.* 53, 4603–4614. doi: 10.1021/jm100210p
- Porta, E. O., Carvalho, P. B., Avery, M. A., Tekwani, B. L., and Labadie, G. R. (2014). Click chemistry decoration of amino sterols as promising strategy to developed new leishmanicidal drugs. *Steroids* 79, 28–36. doi: 10.1016/j.steroids.2013.10.010
- Porta, E. O. J., Jäger, S. N., Nocito, I., Lepesheva, G. I., Serra, E. C., Tekwani, B. L., et al. (2017a). Antitrypanosomal and antileishmanial activity of prenyl-1,2,3-triazoles. *Med. Chem. Comm.* 8, 1015–1021. doi: 10.1039/C7MD00008A
- Porta, E. O. J., Vallejos, M. M., Bracca, A. B. J., and Labadie, G. R. (2017b). Experimental and theoretical studies of the [3,3]-sigmatropic rearrangement of prenyl azides. *RSC Adv.* 7, 47527–47538. doi: 10.1039/C7RA09759J
- Qosa, H., Mohamed, L. A., Alqahtani, S., Abuasal, B. S., Hill, R. A., and Kaddoumi, A. (2016). Transporters as drug targets in neurological diseases. *Clin. Pharmacol. Ther.* 100, 441–453. doi: 10.1002/cpt.435
- Rohloff, P., Rodrigues, C. O., and Docampo, R. (2003). Regulatory volume decrease in *Trypanosoma cruzi* involves amino acid efflux and changes in intracellular calcium. *Mol. Biochem. Parasitol.* 126, 219–230. doi: 10.1016/S0166-6851(02)00277-3
- Rostovtsev, V. V., Green, L. G., Fokin, V. V., and Sharpless, K. B. (2002). A stepwise huisgen cycloaddition process: copper(I)-catalyzed regioselective “ligation” of azides and terminal alkynes. *Angew. Chem. Int. Ed. Engl.* 41,

- 2596–2599. doi: 10.1002/1521-3773(20020715)41:14<2596::AID-ANIE2596>3.0.CO;2-4
- Sayé, M., Fargnoli, L., Reigada, C., Labadie, G. R., and Pereira, C. A. (2017). Evaluation of proline analogs as trypanocidal agents through the inhibition of a *Trypanosoma cruzi* proline transporter. *Biochim. Biophys. Acta-Gen. Subj.* 1861, 2913–2921. doi: 10.1016/j.bbagen.2017.08.015
- Sayé, M., Gauna, L., Valera-Vera, E., Reigada, C., Miranda, M. R., and Pereira, C. A. (2020). Crystal violet structural analogues identified by in silico drug repositioning present anti-*Trypanosoma cruzi* activity through inhibition of proline transporter TcAAAP069. *PLoS Negl. Trop. Dis.* 14:e0007481. doi: 10.1371/journal.pntd.0007481
- Sayé, M., Miranda, M. R., Di Girolamo, F., De Los Milagros Cámara, M., and Pereira, C. A. (2014). Proline modulates the *trypanosoma cruzi* resistance to reactive oxygen species and drugs through a novel D, L-proline transporter. *PLoS ONE* 9:e92028. doi: 10.1371/journal.pone.0092028
- Sayé, M., Reigada, C., Gauna, L., Valera-Vera, E. A., Pereira, C. A., and Miranda, M. R. (2019). Amino acid and polyamine membrane transporters in *Trypanosoma cruzi*: biological function and evaluation as drug targets. *Curr. Med. Chem.* 26, 6636–6651. doi: 10.2174/0929867326666190620094710
- Schneider, C. A., Rasband, W. S., and Eliceiri, K. W. (2012). NIH image to imageJ: 25 years of image analysis. *Nat. Methods* 9, 671–675. doi: 10.1038/nmeth.2089
- Silber, A. M., Colli, W., Ulrich, H., Alves, M. J., and Pereira, C. A. (2005). Amino acid metabolic routes in *Trypanosoma cruzi*: possible therapeutic targets against Chagas' disease. *Curr. Drug Targets Infect. Disord.* 5, 53–64. doi: 10.2174/1568005053174636
- Silber, A. M., Tonelli, R. R., Lopes, C. G., Cunha-E-Silva, N., Torrecilhas, A. C. T., Schumacher, R. I., et al. (2009). Glucose uptake in the mammalian stages of *Trypanosoma cruzi*. *Mol. Biochem. Parasitol.* 168, 102–108. doi: 10.1016/j.molbiopara.2009.07.006
- Silber, A. M., Tonelli, R. R., Martinelli, M., Colli, W., and Alves, M. J. M. (2002). Active transport of L-proline in *trypanosoma cruzi*. *J. Eukaryot. Microbiol.* 49, 441–446. doi: 10.1111/j.1550-7408.2002.tb00225.x
- Sylvester, D., and Krassner, S. M. (1976). Proline metabolism in *Trypanosoma cruzi* epimastigotes. *Comp. Biochem. Physiol. B: Biochem. Mol. Biol.* 55, 443–447. doi: 10.1016/0305-0491(76)90318-7
- Thompson, A. S., Humphrey, G. R., Demarco, A. M., Mathre, D. J., and Grabowski, E. J. J. (1993). Direct conversion of activated alcohols to azides using diphenyl phosphorazidate. A practical alternative to Mitsunobu conditions. *J. Org. Chem.* 58, 5886–5888. doi: 10.1021/jo00074a008
- Tonelli, R. R., Silber, A. M., Almeida-De-Faria, M., Hirata, I. Y., Colli, W., and Alves, M. J. M. (2004). L-Proline is essential for the intracellular differentiation of *Trypanosoma cruzi*. *Cell. Microbiol.* 6, 733–741. doi: 10.1111/j.1462-5822.2004.00397.x
- Tron, G. C., Pirali, T., Billington, R. A., Canonico, P. L., Sorba, G., and Genazzani, A. A. (2008). Click chemistry reactions in medicinal chemistry: applications of the 1,3-dipolar cycloaddition between azides and alkynes. *Med. Res. Rev.* 28, 278–308. doi: 10.1002/med.20107
- Urbina, J. A. (2010). Specific chemotherapy of Chagas disease: Relevance, current limitations and new approaches. *Acta Trop.* 115, 55–68. doi: 10.1016/j.actatropica.2009.10.023
- Yu, X.-C., Zhang, W., Oldham, A., Buxton, E., Patel, S., Nghi, N., et al. (2009). Discovery and characterization of potent small molecule inhibitors of the high affinity proline transporter. *Neurosci. Lett.* 451, 212–216. doi: 10.1016/j.neulet.2009.01.018

Conflict of Interest: The authors declare that the research was conducted in the absence of any commercial or financial relationships that could be construed as a potential conflict of interest.

Copyright © 2020 Fargnoli, Panozzo-Zéner, Pagura, Barisón, Cricco, Silber and Labadie. This is an open-access article distributed under the terms of the Creative Commons Attribution License (CC BY). The use, distribution or reproduction in other forums is permitted, provided the original author(s) and the copyright owner(s) are credited and that the original publication in this journal is cited, in accordance with accepted academic practice. No use, distribution or reproduction is permitted which does not comply with these terms.